Raquel Alexandra Antunes Barras

Licenciada em Engenharia de Micro e Nanotecnologias

Cellulose-based composites as functional conductive materials for printed electronics

Dissertação para obtenção do Grau de Mestre em
Engenharia de Micro e Nanotecnologias

Orientador: Doutor Luís Miguel Nunes Pereira, Professor Auxiliar, Faculdade de Ciências e Tecnologia da Universidade Nova de Lisboa

Co-orientador: Bruno Ricardo Quintino Nunes Pereira, Engenheiro, FISIPE

Júri:

Presidente:	Professor Doutor Rodrigo Ferrão de Paiva Martins
Arguente:	Doutora Lídia Sofia Leitão Santos
Vogal:	Professor Doutor Luís Miguel Nunes Pereira

FACULDADE DE CIÊNCIAS E TECNOLOGIA
UNIVERSIDADE NOVA DE LISBOA

Setembro 2015

Cellulose-based composites as functional conductive materials for printed electronics

© Raquel Alexandra Antunes Barras

Faculdade de Ciências e Tecnologia

Universidade Nova de Lisboa

ACKNOWLEDGMENTS

É com um grande sentimento de satisfação e realização pessoal que entrego este trabalho. Estes ultimos meses foram sem duvida os mais importantes do meu percurso académico e concluir o curso a lembrar-me do primeiro pensamento ao ver a colocação ("entrar foi fácil, sair vamos ver") é também um grande alivio! Este é o fechar de um ciclo de trabalho que não se fez sozinho e por isso não posso deixar de agradecer a todos os que direta ou indireta fizeram parte dele.

Em primeiro lugar agradeço ao professor Rodrigo Martins e à professora Elvira Fortunato pela oportunidade de trabalhar neste centro de excelência que é o CENIMAT.

Deixo um agradecimento especial ao meu orientador Luís Pereira pela excelente oportunidade oferecida, por toda a orientação, ajuda e ideias, pelas reuniões semanais e almoços que contribuiram muito para a união e motivação de todos enquanto grupo. Este espirito de equipa foi muito importante. Por isto tudo, muito obrigada!

Agradeço ao meu co-orientador o Eng. Bruno Pereira, ao Eng. Paulo Correia e à FISIPE pelo material fornecido pois sem ele realizar este trabalho não teria sido possivel.

Agradeço a toda a equipa do CENIMAT e DCM que se revelaram sempre prestáveis para ajudar em qualquer altura: Alexandra Gonçalves, Rita Branquinho, Tomás Calmeiro, Sónia Pereira, Ana Pimentel, Joana Pinto, Daniela Salgueiro, Cristina Fernades, Carolina Marques, Ana Santa, Pedro Barquinha, Rui Igreja, Carlos Dias, Coro Echeverria, Asal Kiazadeh, Jonas Deuermier, Dona Antónia, Marta Ferreira, António Vicente, Ricardo Ferreira e Tiago Mateus. A estes ultimos, muito obrigada pela máquina de *bending*! Diana Gaspar, muito obrigada também por toda a ajuda ao longo do trabalho e antes dele, não fosse MCP e não estaria aqui provavelmente.

Um agradecimento especial aos meus amigos e colegas de laboratório, Paul, Tiago, Pedro, Manu e Inês. Melhor grupo não podia ter calhado, foi tão bom ter passado estes meses convosco. Obrigada por toda a ajuda e paciência.

Em especial agradeço à Inês. A tua ajuda foi muito importante. Se no inicio não via isso, agora nada faz mais sentido. Nada se faz sozinho e se duvidas houver estamos cá nós para contar a história. És uma excelente amiga. Um enorme obrigada é pouco pela tua ajuda em tudo, pelos teus planos de trabalho, pelas aulas de inglês (!) e por me teres aturado principalmente.

A todos os meus colegas de curso, para chegar aqui não vim sozinha, a vossa ajuda foi muito importante, por isso agradeço-vos a todos. Em especial à Ana, mais que tudo és a amiga que está sempre lá. Bea, tu também.

Aos meus pais e irmãos Ricardo, Rita e Rafa, vocês são o motivo disto tudo, seja como for. Vêm em ultimo mas são os que importam mais. Obrigada por todo o apoio incondicional. Adoro-vos. Este trabalho dedico-o a vocês.

Íris, pertences ao parágrafo anterior mas coloquei-te estratégicamente a seguir ao "Adoro-vos", porque já sabes que não estou para isto. Obrigada por tudo, sei que vais estar sempre aí e eu aqui, de preferência não muito longe, por mais chata que sejas e menos paciência que eu tenha.

ABSTRACT

In this work, cellulose-based electro and ionic conductive composites were developed for application in cellulose based printed electronics. Electroconductive inks were successfully formulated for screen-printing using carbon fibers (CFs) and multi-walled carbon nanotubes (MWCNTs) as conductive functional material and cellulose derivatives working as binder. The formulated inks were used to fabricate conductive flexible and disposable electrodes on paper-based substrates. Interesting results were obtained after 10 printing passes and drying at RT of the ink with 10 % wt. of pristine CFs and 3% wt. of carboxymethyl cellulose (CMC), exhibiting a resistivity of 1.03 Ωcm and a resolution of 400 µm. Also, a resistivity of 0.57 Ωcm was obtained for only one printing pass using an ink based on 0.5 % wt. MWCNTs and 3 % wt. CMC.

It was also demonstrated that ionic conductive cellulose matrix hydrogel can be used in electrolyte-gated transistors (EGTs). The electrolytes revealed a double layer capacitance of 12.10 μFcm^{-2} and ionic conductivity of $3.56x10^{-7}$ Scm^{-1}. EGTs with a planar configuration, using sputtered GIZO as semiconducting layer, reached an ON/OFF ratio of $3.47x10^{5}$, a V_{ON} of 0.2 V and a charge carrier mobility of 2.32 $cm^2V^{-1}s^{-1}$.

Keywords: carbon fibers, multi-walled carbon nanotubes, cellulose, electric and ionic conduction, electrolytes, electrolyte-gated transistor, printed electronics, screen-printing.

RESUMO

Neste trabalho foram desenvolvidos compósitos celulósicos com condutividade eléctrica e iónica para aplicação em electrónica impressa e baseada em celulose. Foram formuladas com sucesso tintas electrocondutoras para *screen printing* usando fibras de carbono (CFs) e nanotubos de carbono do tipo multi-walled (MWCNTs) como elementos funcionais para a condução eléctrica e derivados de celulose com a função de espessantes. As tintas formuladas foram usadas para fabricar electrodos condutores flexiveis e descartáveis em substratos derivados de papel. Foram obtidos resultados interessantes após 10 camadas impressas e secas à temperatura ambiente usando uma tinta composta por 10 % wt. de CFs sem tratamento e 3 % wt. de carboximetilcelulose (CMC), com uma resistividade de 1.03 Ωcm e uma resolução de 400 µm. Conseguiu-se ainda uma resistividade de 0.57 Ωcm para apenas uma camada impressa com a tinta de 0.5 % wt. de MWCNTs e 3 % wt. de CMC.

Demonstrou-se ainda a aplicação de matrizes celulósicas de condutores iónicos na forma de hidrogéis em transístores do tipo *electrolyte-gated* (EGTs). Os electrólitos apresentaram uma capacidade de double layer de 12.10 μFcm^{-2} e uma condutividade de $3.56x10^{-7}$ Scm^{-1}. Os EGTs, de configuração planar e com uma camada semicondutora de GIZO alcançaram um rácio de corrente ON/OFF de $3.47x10^{5}$, uma tensão V_{ON} de 0.2 V e uma mobilidade de portadores de carga de 2.32 $cm^2V^{-1}s^{-1}$.

Palavras-chave:fibras de carbono; nanotubos de carbono, celulose, condução eléctrica e iónica, electrólitos, *electrolyte-gated transistors*, electrónica impressa, *screen-printing.*

LIST OF ABBREVIATIONS

3D – Three dimensional
a.u. – Arbitrary units
AA – Acetic acid
AC – Alternate current
AgNW – Silver nanowire
BNC – Bacterial cellulose
C – Capacity
CA – Cellulose acetate
CEMOP – Centro de Excelência de Microelectrónica, Optolectrónica e Processos
CENIMAT | i3N – Centro de investigação de materiais/ Instituto de nanoestruturas, nanomodelação e nanofabricação
CF – Carbon fiber
CMC – Carboxymethyl cellulose
CNT – Carbon nanotube
CV – Cyclic voltametry
DMF – N_2O_4/N,N-dimthylformamide
DSC – Differential scanning calorimetry
EC – Ethyl cellulose
ECT – Electrochromic transistor
EDL – Electrical double layer
EDLT – Electrical double layer transistor
EGT – Electrolyte gated transistor
EIS – Electrochemical impedance measurement
EtOH – Ethanol
FET – Field effect transistor
FIB – Focused ion beam
FS2 – Felix Schoeller type 2 paper
FS3 – Felix Schoeller type 3 paper
FTIR – Fourier transform infrared spectroscopy
FWHM – Full width at half maximum
GIZO – Gallium indium zinc oxide
HPC – Hidroxypropil cellulose
ITO – Thin-doped indium oxide
MCC – Microcrystalline cellulose
MW – molecular weight
M_w – Molecular weight
MWCNT – Multi-walled carbon nanotube
NCC – Nanocrystalline cellulose
NFC – Nanofibrillated cellulose
NMMO – N-methylmorpholine-N-oxide monohydrate
NP – Nanoparticle
NW – Nanowire
PAN – Polyacrilonitrile
PANI-rGO – Polyaniline reduced graphene oxide
PC – Polycarbonate
PEG – Polyethylene glycol
PEO – Polyethylene oxide
PET – Polyethylene terephtalate
PI – Polyimide
PVD – Physical vapor deposition
R2R – Roll to roll
RFID – Radio frequency identification tags
RH – Relative humidity
RMS – Root mean square
RT – Room temperature
SEM – Scanning electron microscope
SWCNT – Single walled carbon nanotube

TFT – Thin film transistor
TGA – Thermal gravimetric analysis
Tol – Toluene
U – Urea
UV – Ultraviolet
X-ray – X radiation
XRD – X-ray diffraction

LIST OF SYMBOLS

θ – Angle
λ – Wavelength
ρ – Resistivity
σ – Conductivity
σ_i – Ionic conductivity
ω – Angular frequency
C_b – Bulk capacitance
C_D – Electrical double layer capacitance
d – Thickness
I_{DS} – Drain-source current
I_{GS} – Gate-source current
I_{OFF} – Off state electrical current
I_{ON} – On state electrical current
$I_{ON/OFF}$ – On/Off current ratio
L – Channel length
n – Refraction index
V_D – Drain voltage
V_G – Gate voltage
Z – Impedance

TABLE OF CONTENTS

LIST OF FIGURES

LIST OF TABLES

1. Motivation and objectives

1.1. Motivation

Nowadays, there is a growing interest in the area of printed electronics as an alternative to conventional silicon-based electronics. Printed electronics is focused on the development of new low-cost, simple, versatile electronic components and devices through high throughput deposition processes. The implementation of printing techniques on flexible substrates, like plastic foils and cellulose paper, assumes great importance, especially the last when sustainability and recyclability are considered. [1]

Paper is a cheap, ubiquitous, and biofriendly material composed of cellulose fibers that are used as a flexible substrate for many applications in daily life. [2] The strong interest among the scientific and industrial community in the production of electronic or electrochemical devices on cellulose paper substrates is mainly driven by its low cost, lightweight, flexibility and ability to be 100% recyclable. [3] Additionally, cellulose itself is a renewable, biodegradable and the most abundant biopolymer resource available on Earth, with a low environmental impact, being for these reasons considered into a class of materials that may be adapted for the development of innovative electronic composites with new functionalities. [2][4]

Nevertheless, dissolution of cellulose remains a challenge, due to its rigid long-chain and strongly inter-molecular and intra-molecular hydrogen-bonded structure. For this reason, cellulose is usually converted into derivatives, such as sodium carboxymethyl cellulose (CMC) and ethyl cellulose (EC), with interesting properties [5]. Anyhow, several kinds of solvent systems have been developed to prepare new regenerated cellulose [6]. Aqueous alkali hydroxide solutions combined with urea, thiourea, urea/thiourea or PEG have been reported in the literature [7]–[10] as promising solvent systems for cellulose dissolution, due to their simplicity, low cost, low toxicity and rapidity, producing cellulose hydrogels without any hazardous byproducts.

In CENIMAT, paper and electronics have been crossing common paths, with pioneer work being developed on using cellulose paper as substrate for solar cells [11][12], batteries [13], colorimetric sensors [14], and also as gate dielectric in field effect transistors (FETs) [3], [15]–[17]. More recently, the combination of printing techniques with paper as a physical support has been explored for the development of thin film transistors (TFTs) [18], digital microfluidics [19]–[21] electrochromic displays and gas sensors.

Research regarding the exploration of new functional materials based on cellulose became a hot topic. However, not much can be found in the literature about the use of cellulose as an active material in printed electronics, which presents one of the main motivations for the present work.

The hydrophilic nature of cellulose and its ability to form films and hydrogels makes it suitable to act as carrier, matrix or scaffold in new functional materials. Most of the efforts are devoted to the development of composites, where cellulose or its derivatives are combined (through doping, blending or coating) with conductive functional materials, such as carbon structures, conductive polymers, ionic liquids, metal ions and oxides, giving rise to materials with new properties in the form of microspheres, fibers or membranes. [22]

This work aims to bring new insights in cellulose composites. This master thesis is focused on the development and study of cellulose-based composites either as functional electroconductor or ionic conductor materials. The ultimate goal relies in advancing the state-of-the-art in the area of printed electronics, implementing the developed cellulose-based composites.

The use of functional materials, such as electroconductive, based on carbon fibers (CFs) or multi-walled carbon nanotubes (MWCNTs), demands the formulation of suitable inks, which consists in a mixture of the conducting material in a solvent and various additives. Furthermore, it is critical to find the best combination between each component, in order to provide optimal printability combined with high electrical conductivity. Preparation of such inks is challenging, even more when high viscosity is required, as for screen printing, since this condition is only achieved through the addition of polymer binders, like cellulose derivatives (for instance, CMC and EC) that, being non-conducting materials will negatively affect the electrical performance.

Additionally, there are some concerns related to the development of MWCNTs- and CFs-based electroconductive inks, due to their tendency to be in the form of large bundles or ropes [23]. Although, there are several attempts in order to obtain a stable dispersion of the carbon structures in the dispersing medium. [24] The use of cellulose derivate as dispersants was already demonstrated [25] and CMC was

successfully used as excellent dispersant of single-walled CNTs (SWCNTs), in terms of stability, high concentration, versatility and film-forming ability. [26]

Taking these considerations into account, cellulose-based electroconductive composite inks were synthesized and formulated with the technical specifications for screen-printing, using a simple and eco-friendly method by blending carbon structures, such as CFs and MWCNTs, into the matrix of a cellulose derivative. EC and CMC were selected as dispersing and stabilizing agents of the carbon structures due to their high viscosity, which enables their use as binders for screen-printing. CFs were selected as conductive functional material thanks to their relatively low cost for industrial scale production (if compared to CNTs) and high availability [27][28]. Nevertheless, CFs are very long (> 100 µm) as compared to CNTs (< 10 µm), which complicates their printability and solution dispersion and stabilization [29]. Thus, mechanical treatments can be a solution in order to reduce their size, but this approach can significantly alter the morphology and aspect ratio of the CFs, reducing the conductivity of the final composite.

The physical properties of the conductive inks and the structure, morphology and electrical properties of the screen-printed films was also focused. These results were correlated with the influence of paper surface properties (such as roughness, porosity and wettability), blending content and morphology of carbon structures, cellulose derivative used as a binder, drying conditions and number of printing passes on print quality and electrical performance of the printed films. The effect of the bending on electrical properties of the screen-printed films was also examined and discussed.

Concerning the development of cellulose-based electrolytes for application in electrolyte-gated transistors (EGTs), not much can be found in the literature regarding EGTs based on cellulose serving as a gate insulator. These devices are able to operate at low voltages, due to the high capacitance achieved by the formation of electric double layers, a very interesting feature for low cost autonomous systems, exactly the type of applications targeted by “printed electronics”. Moreover the EGTs are of particular interest when using printing techniques on substrates that cannot support high temperatures since the electrolyte does not necessarily need any annealing temperature, unlike most solution based dielectric layers.

In this master thesis, we also report the use of cellulose matrix hydrogel electrolytes produced from dissolution of microcrystalline cellulose (MCC) in aqueous LiOH/urea solvent systems as the dielectric layer of EGTs. Here we adapted the conventional procedure, in order to incorporate lithium ions into cellulose, being the resultant cellulose-based hydrogels suitable electrolytes for this specific application.

1.2. Objectives

The work developed in this master thesis is focused on the development and study of eco-friendly conductive composites based on cellulose, aiming their application as functional layers of printed devices. Two different cellulose composites were designed and engineered based on microcrystalline cellulose (MCC) and cellulose derivatives, such as CMC and EC, which were used as matrix of ionic conductors and electroconductive functional materials based on carbon structures, respectively.

Concerning the development of cellulose-based composites as functional electroconductive material, several studies were performed in order to find the optimal ink composition and screen-printing conditions with the final goal of developing an electroconductive printed pattern. This topic involves the following studies:

- Structural, morphological and electrical characterization of the carbon structures;
- Physical properties of the formulated inks and their optimization;
- Surface properties and thermal stability analysis of different paper substrates;
- Optimal conditions for fabrication of screen-printed conductive patterns;
- Electrical characterization of the screen-printed conductive patterns;

For the development of cellulose-based composites as ionic conductor materials, this topic will be divided into the following sub-objectives:

- Preparation of a cellulose matrix hydrogel electrolyte from MCC, using a simple, fast, low cost and less toxic dissolution method based on aqueous alkali/urea solvent systems;
- Electrochemical characterization of the electrolytes;
- Application of electrolytes in EGTs.

2. GENERAL INTRODUCTION

For a better understanding of this work, a brief introduction will be given in this section, comprising subjects, such as fundamentals and applications of printed electronics and cellulose. Depending on the functionality, the latter topic is divided into cellulose-based composites either as functional electroconductive materials, incorporating carbon structures such as carbon fibers and multi-walled carbon nanotubes (MWCNTs), or as ionic conductive materials, being some attention given to electrochemical devices, like electrolyte-gated transistors (EGTs).

2.1. Printed electronics: fundamentals and applications

Over the past recent years, research in the area of printed electronics tried to reply to the increasing demand on low-cost, high volume and high-throughput production of lightweight, small, thin, flexible, cheap and disposable electronic components or devices. It's not a real novelty that most of traditional printing techniques have been adopted for printed electronics. There are reports since before 1950 of using ink solutions and printing techniques to produce circuits on wiring boards. [30] Despite this technology has been surpassed by more accurate deposition techniques back then, the today's needs on low cost, disposable and flexible technology that cannot be fulfilled by silicon-based electronics are slowly bringing printing electronics back to life. [31]

Fabrication of traditional electronic devices requires the use of vacuum and high temperatures, corrosive chemicals and expensive, sophisticated equipment and infrastructures. Rigid materials, such glass [32] or silicon [33], are often used as substrates because the exposition to such conditions usually are not compatible with the use of flexible substrates, like paper and plastic foils. [34] The possibility of using new deposition methods, such as printing techniques, that don't require vacuum conditions and can be processed at low temperatures brings great advantages in matter of energy consumption and complexity, opening a new world of low-cost printed circuits based on conductive, semiconductive and dielectric printed materials. [31]

Table 2.1 compares parameters of several printing techniques that can be adapted for printed electronics. For instance, it is possible to obtain a very high definition of patterns using nanoimprint technique, while fast printing speeds are achieved using offset and gravure printing. However, such techniques require complex equipment's that are more suitable for industrial scale production. Also, inkjet is a simple and cheap technique that allows precise patterning with reduced raw material waste, but the nozzle limits the particles size to very small dimensions (in the order of the dozen of nm) [35]. For a laboratorial scale, screen printing, which will receive further attention in sub-section 1.1.1.,stands out as a promising printing technique, due to its simplicity, adaptability and reliability even when performed manually on an affordable and homemade system.[30]Moreover, screen printing is also scalable to industrial level and compatible with roll-to-roll (R2R) processing.[36] For these reasons, screen printing was selected for development of films with different functionalities, receiving great attention along this work.

Table 2.1 – Comparison of some features between several printing technics that can be adapted to printed electronics.[30]

	Viscosity (cp)	Line width (μm)	Line Thickness (μm)	Speed (m/min)
Inkjet	10 – 20	30 - 50	~ 1	~ 60
Offset	100 - 10000	~ 10	< 10	~ 1000
Gravure	100 - 1000	10 - 50	~ 1	~ 1000
Screen	50 - 5000	30 - 50	5 - 100	~ 500
Nanoimprint	-	~ 0,01	~ 0,1	(Slow)

In addition to the ease of process offered by printing technologies, the natural choice of using plastic foils or paper as flexible substrates and the ability for deposition in large areas are also advantages.[31]Most common materials used in flexible electronics are polymers, like polyethylene terephthalate (PET) [31], polycarbonate (PC) [31], polyimide (PI) [31] or cellulose-based substrates[37].

In particular, paper and cellulose-based substrates have unique characteristics among other flexible substrates, such as the abundance and low cost of cellulose as raw material, associated with its properties of being biodegradable, renewable and recyclable. [34][37] Nevertheless, paper exhibits a porous structure and a large surface roughness, with peak-to-valley roughness values of up to hundreds of micrometers, with a series of shortcomings to hosting electronic devices on its surface associated to its high absorbency. [37][38] Thus, paper is a challenging substrate compared to smooth but more expensive and non-biodegradable plastic sheets. [2][4] Countless devices rely on printed electronic technologies, exploiting the potential of paper as a substrate, such as resistors[34], photovoltaic cells [39], transistors [2][34], radio frequency identification tags (RFIDs) [1], sensors [39] and pharmaceutical applications [40].

Figure 2.1a-e shows some examples of electronic devices developed in CENIMAT, where paper is used as the physical support (Figure 2.1a), substrate for solar cells (Figure 2.1b) [11][12] and batteries (Figure 2.1b) [13]. More recently, paper has been exploited as substrate for printed electronics, developing thin film transistor (TFT) devices (Figure 2.1d) and electrochromic displays for gas sensors (Figure 2.1e).

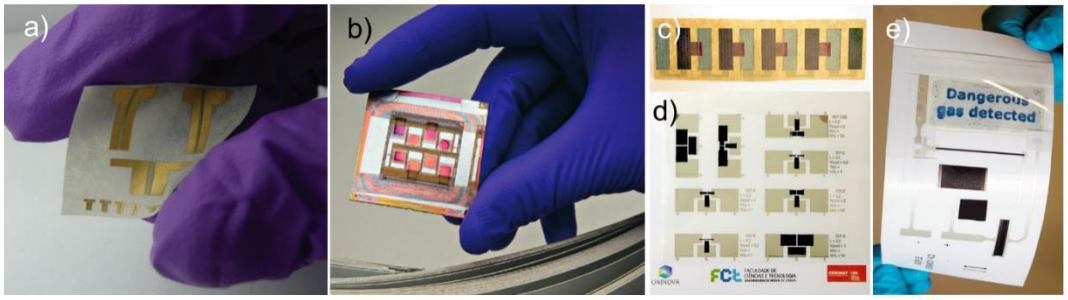

Figure 2.1 –CMOS technology with cellulose paper working as substrate and dielectric of n and p-type FETs[17][41](a); Solar cell on Tetra Pack® substrate deposited by physical vapor deposition (PVD) techniques [12] (b); bio-batery on paper substrate[13] (c); screen printed TFTs on cellulose substrate[Adapted from [42]] (d); Screen printed electrochromic display for gas sensing on cellulose cubstrate [Adapted from [43]] (f).

2.1.1. Screen Printing

A simple screen printing system [30], as illustrated in Annex A, consists of a flat support with a patronized screen within frame. The support holds the frame and substrate to be printed and also gives stability to the whole structure; the screen made of polyester fibers or stainless steel mesh with an announced thread diameter and aperture is patronized using a photosensitive resin, which after curing forms permeable and not permeable areas over the mesh fibers. The printing technique consists of spreading an amount of ink through the screen with the help of a squeegee, allowing the ink to pass throw the permeable areas and form the desired pattern in the substrate. Screen printing technique allows the printing of patterns of minimum 10 µm, with thickness ranging from 5 to 100 µm, depending on the mesh size and ink composition. [30][35][44]

The quality of printing patterns relies on a number of parameters related with the screen mesh properties, intrinsic ink characteristics, printing speed and external factors embracing the operator. Although in an automatic screen printing machine these factors are well controlled, the same doesn't happen for manual screen printing.

In a two dimensional point of view, the thread diameter and aperture dictates the maximum resolution that can be achieved. Since small openings within small distance allows more details to be distinguished, resolution factor in inversely proportional to mesh opening and aperture, and a small mesh is what one looks for when searching for good resolution. The film thickness is also greatly influenced by these parameters.

Moreover, ink rheological properties like viscosity, mass content and contact angle with the substrate are also important. Annex B shows the usual values for shear rates applied to the ink on each printing step (from 10^{-2} to 10^{3} s^{-1}) and the typical viscosities for screen printing inks. It's very important that ink behavior adapts to each stage of the printing process: (1) the ink should exhibit shear thinning behavior when the tangential stress is applied; (2) viscosity should be low enough to allow flowing through the mesh, and (3) after tangential stress have been removed and the ink have been deposited on the substrate, the recovery should exhibit a thixotropic character. [45][46] To achieve such characteristics, ink composition is generally a combination of [46]:

- Active elements: responsible for the functional properties;
- Solvent: the vehicle for transport and dispersion of the active element;
- Binders (or thickeners): used to adjust rheological properties and after curing or drying time, are responsible for incorporating the active element on the solid matrix;
- Additives: used to adjust properties, like wettability or surface tension, and improve particle dispersion and stability in the solvent, or even to improve properties in the printed film like porosity after sintering step.

Additionally, external factors, such as speed of squeegee and applied force to spread the ink, are also considered. The combination on these factors are traduced in a measurable parameter, the shear rate, along whose the viscosity of ink varies.

2.2. Cellulose

Social conscience and economic factors are great concerns for today's consumers and society in general. The combination of eco-friendly and low cost materials are specially desired qualities in the search for new products and, among a wide range of raw materials, biopolymers seems to satisfy both. [47]

Biopolymers are natural occurring polymers, with its origin on living organisms although they can also be obtained by chemical processes. [47] Starch, cellulose, chitosan, gelatin and chitin are some examples of natural occurring biopolymers, among whose cellulose is the most explored. [47]

Cellulose is a renewable and biodegradable biopolymer and the most abundant on Earth, and can be found in plant cell walls, which is the main source, some sea organisms, fungi and bacteria. It is estimated that per year, the amount of available resources reaches 10^{11} tons, which falls far short from limits of production (only about 2%). [48] For that fact, this raw material has a great value for industry. It's biocompatibility, high elastic modulus, thermal stability, nontoxicity and low density makes it suitable for a wide range of applications, from paper and textile, food, pharmaceutical and chemical industry to disposable electronics. [48]

Figure 2.2 shows the organization of the hierarchical structure of cellulose. When extracted from plants, cellulose can be found in cell walls in the form of crystalline microfibrils, along with randomly organized hemicellulose. The cellulose molecule is constituted by D-anydroglucopyranose units, linked by β glycosidic bonds and assembled into groups of cellobiose units. The hydroxyl groups along the polymer chain skeleton forms inter bonds, responsible for the microfibrils of crystalline structure, with lateral dimensions of 5 to 10 nm and several micrometers long.[48][49] In these crystalline regions, according with the molecular orientation, cellulose can form different types of allomorphs. The most commonly form found in nature is cellulose I, where all the molecules have the reducing and non-reducing end in the same direction (parallel), with subalomorphs Iα and Iβ presenting a triclinic and a monoclinic structure, respectively. Cellulose II has antiparallel chains and it's the more stable form of cellulose. Another less occurring allomorphs are cellulose III and IV, which can be obtained from the previous forms. [47]

The possibility of manipulation of cellulose at the nanoscale to form nanostructured materials allows the combination of important cellulose properties with large superficial area. The most important nanostructures of cellulose are micro or nanofibrillated cellulose (MFC/NFC), nanocrystalline cellulose (NCC) and bacterial nanocellulose (BNC). The use of fibers with inferior diameter dimensions than the wavelength of light brings also advantages for optical properties, resulting in transparent cellulose composite materials with a lot of promising applications. [50]

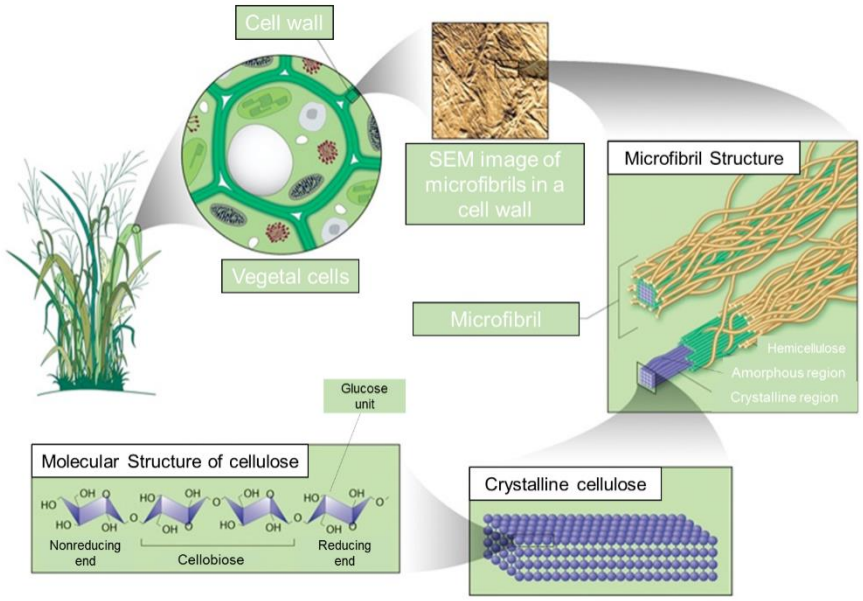

Figure 2.2 – Scheme of hierarchical and chemical structure of cellulose from vegetal origin (Adapted from [51]).

The hydrogen bonds responsible for the partial crystalline structure of cellulose, and the dense packaging of these regions difficult dissolution of cellulose, which is not soluble in water neither in common organic solvents. The most common used solvent systems are lithium chloride/dimethyl sulfoxide (LiCl/DMSO) [52], lithium chloride/N,N-dimethylacetamide (LiCl/DMAc) [53], N_2O_4/N,N-dimthylformamide (DMF) [53], N-methylmorpholine-N-oxide monohydrate (NMMO) [53] and ionic liquids [53], but they are limited to laboratory scale applications, due to volatility, toxicity and high cost. [10]

Recently, Zhangs's group [10] developed a simple and rapid method based on inexpensive and less toxic solvent systems for cotton linter dissolution at low temperatures thus producing cellulose hydrogels. This approach consists of dissolution of cellulose in aqueous alkali hydroxide solvents systems, such as NaOH/urea [7][8][9], NaOH/thiourea [8], NaOH/Urea/Thiourea [54] and LiOH/Urea [8][9]. Briefly, cellulose is dissolved at low temperatures (between -5 and -12ºC[8]) in the pre-cooled solvent system, under vigorous stirring, and then regenerated in a coagulation bath (such as, ethanol, acetone, t-butanol and aqueous solutions of 5 % wt. H_2SO_4 or 5 % wt. H_2SO_4: 5 % wt. Na_2SO_4[9]). Finally, the hydrogel of regenerated cellulose is washed with deionized water to remove the residual chemical reagents and dried, obtaining transparent and bendable cellulose films with gas barrier properties. Nevertheless, these systems are not able to dissolve cellulose at room temperature conditions and the precise structure of the dissolution mechanism involved is not fully understood. [54][7][8][9]

Alternatively, the substitution of hydroxyl groups by other functional groups results in derivatives of cellulose that are easily dissolved in ordinary solvents and doesn't need such complex systems. [48] Some examples are ethyl cellulose (EC), hydroxypropyl cellulose (HPC), methyl cellulose (MC), sodium carboxymethyl cellulose (CMC) and cellulose acetate (CA), with a wide range of applications on food, pharmaceutical and cosmetic industry.[5]

The possibility of dissolution of cellulose compounds and its derivatives, and the incorporation of particles with key properties, led to the creation of functional materials that will be discussed in the next sub-sections.

2.2.1. Cellulose composite as functional electroconductive material

The hydrophilic nature of cellulose and its ability to form films and hydrogels makes it suitable to act as carrier, matrix or scaffold in new functional materials. [22] In particular, cellulose electroconductive materials can be obtained by the addiction of inorganic nanoparticles, metal ions and oxides, carbon micro and nanostructures and conductive polymers. Despite most commonly used electroconductive materials are able to achieve great conductivity values [24], they are often too expensive, harmful for the environment or even hard to disperse and stabilize, requiring additional treatments, such as functionalization or the use of surfactant agents. The long chain of cellulose molecules assure the dispersion and stability of these compounds in solution and allows the combination

of electroconductive properties with high hydration, swellability and biocompatibility properties inherent of cellulose compounds.[22] In fact, it was found that the dispersing ability of CMC is twenty times higher than commonly used dispersing agents as sodium dodecyl sulphate (SDS), in the case of SWCNTs. [26]

There are several methods to combine cellulose with conductive materials by blending, coating or doping with the cellulose fibers, being the electroconductive material dispersed on the surface or within the cellulose matrix.[22]Recent work has been developed involving the preparation of these composites, such as conductive and uniformly connected networks of cellulose nanofibers with CNTs and silver nanowires for transparent paper electronics[55], polyaniline reduced graphene oxide coating the surface of cellulose fibers for flexible supercapacitors[56] and CNTs used as doping agent for electrically conductive cellulose aerogels [57].

Although blending cellulose with conductive materials is currently an extremely attractive and advantageous approach, until now not much information can be found about application of this method in printed electronics. So far, Gao and co-workers [25] formulated a stable pristine graphene ink using cyclohexanone and ethyl cellulose, as solvent and stabilizing agent, respectively, which was used to print highly conductive electrodes ($9{,}24 \times 10^3$ Scm^{-1}) onto paper and plastic foils by inkjet printing. However, graphene foils are difficult to obtain and to use in large scale. As an alternative, other carbon allotropes, such as carbon fibers (CFs) and carbon nanotubes (CNTs), seem to be very promising to this kind of applications.

CFs can be obtained from industrial processes by carbonization of organic compound under temperatures ranging from 700 to 2700 ºC [58][59]. Regarding the atomic structure of CFs, carbon atoms are arranged unto a honeycomb like two dimensional matrix, with hydrogen bridges bonding the graphitic layers, which can be arranged in several possible configurations.[60][61] Manufacturing process of FISIPE, the company that provided the CFs used in this work, consist on a oxidation step (200-300 ºC) followed by the carbonization (1200-1400 ºC) of polyacrilonitrile (PAN) for the production of high quality CFs, and the surface treatment before the milling process guarantee a good dispensability, making it ideal for application in mixing processes (Annex C). [62]

CNTs can be described as graphene foils wrapped up on a cylindrical like structure and can be obtained by several methods, like electrical arc discharge, laser ablation or chemical vapor deposition. Unlike CFs, large scale production of CNTs is still a common problem for all those synthesis methods [63]. Like CFs, CNTs atomic structure are arranged in a hexagonal form (graphene walls) and there are two distinct types of CNTs, the single-walled CNTs (SWCNTs) and the multi-walled CNTs (MWCNTs), as illustrated on Annex D. The high conductivity of CNTs is related to electrical conduction along a one-dimensional direction that prevents the influence of lattice defects on electrical resistance present on three-dimensional crystals (as CFs). [64]

Comparing CNTs with CFs, CNTs have a higher electrical conductivity, while CFs have a relatively low cost and availability.[27] However, the dispersion of this structures in a stable solution is not trivial since van der walls forces of attraction causes the formation of bundles and cluster (mostly for MWCNTs, because of its higher aspect ratio). [23] The use of cellulose derivatives as dispersants of carbon structures was already demonstrated [25] and from several attempts in order to obtain stable dispersions solutions [24], EC is already being used in the formulation of many functional inks [44][46][86][87]. In recent studies, CMC also revealed some excellent properties in terms of good isolation, stability and film-forming ability, even for high concentrations of SWCNTs. [26] Based on this, EC and CMC reveals great potential for the successful preparation of electroconductive inks with carbon structures as active element.

2.2.2. Cellulose composite as functional ionic conductive material

Ionic conductive compounds, or electrolytes, are composed by dissociated salts in a solution, forming positive ions (cations) and negative ions (anions). Electrolytes are characterized by an high ionic conductivity and a ideally electrical insulation behavior [4], being responsible for ionic exchanges in a countless type of electrochemical devices, such as batteries and fuel cells, electrolytic capacitors, electrochromic devices [65][66] and electrolyte-gated transistors (EGTs) [66].

Although the typical configuration of electrolytes is in the liquid state, for the most of applications this reveals some issues such as thermal stability at high temperatures, difficulty for large scale production and the possibility of leakage is a real concern. [67] To overcome these issues, great efforts have been made in order to replace liquid electrolytes for gel or solid electrolytes. [67]

An example of solid electrolytes based on cellulose is the study reported by Taichi et al. [68] In this work, it was developed a new class of solid polymer electrolytes that comprise poly (ethylene oxide), poly (cyano acrylate), lithium bis(oxalate)borate and robust cellulose nonwoven for high-performance lithium batteries. The developed electrolyte exhibits outstanding properties, such as high mechanical integrity strength as compared to pristine PEO solid polymer electrolyte, fair ionic conductivity ($3x10^{-4}$ Scm^{-1}) at 60 ºC, and thermostability (up to 160 ºC). The prepared lithium iron phosphate (LiFePO4)/lithium battery using this electrolyte revealed excellent rate capability and high cycling retention, and allowed for a safe and stable operation up to 160 ºC. However, it is often that these devices encountered poor mechanical strength and low ionic mobility (ionic mobility in solids state is limited).

On the other hand, gels present itself as an advantageous alternative, overcoming the problems of ionic conduction in solid electrolytes and partially solving the technical issues of handling in liquid state electrolytes.[69][3] The ability of cellulose to form hydrogels makes it a very interesting alternative for the development of electrolytes and their application in electrochemical devices. [70]

Hydrogels consists of a three-dimensional polymeric network that are able to retain a lot of water on its structure, being H^+ and OH^- ions responsible of the ionic conductivity.[71]The conductivity of the hydrogels can be increased by the addition of salts or metal particles.[72] There are some reports related with the development and application of such cellulose hydrogel electrolytes.

Ramos et al. [71] reported the preparation and characterization of cellulose hydrogels as functional electrolytes, which are based on a combination of Laponite, CMC, poly (acrylic acid sodium salt) and lithium perchlorate, aiming their application in electrochromic windows. These electrolytes exhibited an ionic conductivity at room temperature (25 °C) in the range of 6 to 9 × 10^{-5} Scm^{-1}. It was successfully demonstrated their application in NiO-based electrochromic windows, showing a significant transmittance modulation around 45 % at 600 nm.

New approaches have been made taking advantageous of the dissolution methods of cellulose involving ionic liquids. Thiemann et al. (2014) developed for the first time cellulose hydrogel electrolytes for application in FETs. [4] These electrolytes were obtained by drop casting of methylphosphanate ionic liquids onto microcellulose films, followed by annealing at 80 ºC for 3 h to induce gelation. The cellulose ionogels exhibit interesting properties, such as transparency, flexibility, transferability and high capacitance (5-15 μFcm^{-2}), finding applications in flexible electronics as high capacitance gate dielectrics for EGTs on paper.

Because of the high capacitance of ionic compounds (1-10 μFcm^{-2}) even when compared to high k dielectrics by at least one order of magnitude [3][73], electrolytes are successfully used in specific types of field effect transistors (FET): the electrolyte gated transistors (EGTs). The field effect is the driving force of current modulation in FETs that are constituted by a semiconductor between the drain a source electrodes and the dielectric layer sandwiched between the semiconductor and the gate electrode. [66] EGTs are characterized by replacing the traditional gate dielectric, such as Ta_2O_5 [73], TiO_2 [74], HfO_2 [75], ZrO [76], of conventional FETs by a high capacitance electrolyte. [66]

Depending on the permeability of the semiconductor layer and on the applied gate voltage, EGTs are divided into electrical double layer transistors (EDLTs) or electrochemical transistors (ECTs). [3][73] The presence of a high ionic conductive layer as dielectric in these devices promotes the accumulation of charges on the dielectric/gate and dielectric/semiconductor interfaces. Normally, this leads to the formation of two electrical double layers (EDLs) on each of the interfaces (principle of work of EDLTs). However, when the semiconductor is permeable to ions, reversible electrochemical doping occurs on this layer and only one EDL is formed in the dielectric/gate interface, as the ions are expected to diffuse into the semiconductor (principal of work of ECTs). Comparing these two devices, EGTs finds itself as more interesting than ECTs, since a high leakage current is associated to semiconductor doping. The charge accumulation/depletion in the semiconductor channel is responsible for the modulation behavior of the device. The high capacitance of the electrolytes allows for low operation voltage, being much lower than conventional in conventional thin film transistors (TFTs), which have been attracting much attention for these devices. [73] Moreover, static-capacitance of the electrolyte is thickness independent, giving a high margin to fabricate this device with plenty deposition techniques and on industrial scale, in specific R2R printing on flexible substrates. [73]

3. MATERIALS AND METHODS

3.1. Printable cellulose-based electroconductive composite film for paper electronics

3.1.1. Materials and reagents

CFs and MWCNTs (NC7000) were provided by FISIPE and Nanocyl, respectively. CMC (M_w ~250000) and EC (viscosity 300 cP, 5 % in toluene/ethanol 80:20 (lit.), extent of labeling: 48 % ethoxyl) were purchased from Sigma-Aldrich. Ethanol analytical reagent grade was provided by Fisher Scientific and toluene (≥ 99 %) was purchased from Merck. Deionized water (Millipore) was used.

3.1.2. Mechanical treatments applied to the carbon fibers

CFs were used in three forms: as-received, sonicated and milled. Sonication and manual grinding of CFs were performed in order to reduce fibers length and improve their dispersability and printability. Regarding CFs sonication, an aqueous dispersion of CFs was prepared and ultrasonicated with a cylindrical tip (3 mm end cap diameter) for different times in a UP400S sonicator, using the following parameters: amplitude, 40 %; time on, 2 s; time off, 2 s; time of ultrasonication, 30 min to 6 h. The flask with the aqueous dispersion of CFs was placed in a bath of ice water during sonication, in order to prevent rising of the temperature. Sonicated CFs were dried in a petri dish at 70 ºC until complete evaporation of water.

Milled CFs were obtained by dispersing CFs in an acetone bath, followed by manual grinding in a mortar and drying in a petri dish at 70 ºC until complete evaporation of acetone.

3.1.3. Characterization of carbon fibers and multi-walled carbon nanotubes: structural, morphological and electrical analysis

The morphology of CFs (pristine, milled and sonicated) and MWCNTs was examined by scanning electron microscopy (SEM) using a Carl Zeiss Auriga crossbeam (SEM-FIB) workstation instrument equipped with an Oxford X-ray energy dispersive spectrometer. Samples' preparation procedure for SEM is given in Annex **E**. Due to the length size of the CFs (> 80 μm) an optical microscope (Olympus BX51) equipped with an Olympus DP50 camera and the Cell F View Image System Software was used. The dimensions of CFs and MWCNTs were determined from optical microscope and SEM images, respectively, using ImageJ software.

The structural analysis of the carbon structures was done by X-ray diffraction (XRD) using a PANalyticalX'Pert Pro X-ray diffractometer in Bragg–Brentano geometry, with a monochromatic Cu-Kα radiation source (wavelength 1.5406 Å). XRD measurements were carried out from 10 ° to 65 º (2θ), with a scanning step size of 0.017 °. Also in situ variable temperature XRD measurements were performed from RT until 500 ºC, in order to study thermal stability of pristine CFs.

Electrical characterization of CFs was performed using single ribbon precursors and silver paint as contact and using a multimeter to measure resistance for several ribbon lengths.

3.1.4. Inks formulation for screen-printing

3.1.4.1. Inks formulation

Cellulose-based electroconductive composite inks were formulated by blending carbon structures into a cellulose derivative solution. For CMC-based inks, the carbon material was mixed in different proportions into an aqueous solution of CMC (3 % wt.). The resultant dark dispersion was vigorously stirred for 24 h to ensure complete dissolution of CMC in water and improve carbon structures distribution in the solution. When EC is used as stabilizing and dispersing agent of carbon structures, their dispersion occurs after dissolution of 5 % wt. EC in a mixture of toluene:ethanol (80:20 %v/v), followed by vigorous stirring for 24 h to obtain a dark viscous solution. Tables on Annex F and Annex G summarizes the components and respective weight percentage that were used in the screen-printing inks, using CFs and MWCNTs as conductive functional materials, respectively.

3.1.4.2. Measurement of physical properties of the screen-printing inks

The viscosity of the cellulose/carbon inks was measured on Bohlin Gemini HR^{nano}rheometer, in parallel plates geometry (20 mm diameter and 500 µm gap) for steady-state measurements. Temperature was kept at 25 °C and, before starting the measurements, samples were subjected to a pre-shearing stage, with a pre-shear of 1 s^{-1} applied for 30 s, followed by an equilibration time of 180 s. A solvent trap was used in order to avoid evaporation. The steady-state measurements were performed for shear rates up to 1000 s^{-1}.

To investigate their thermal stability, thermal gravimetric analysis (TGA) of cellulose derivatives solutions and prepared inks were performed using a Simultaneous Thermal Analyzer (TGA-DSC - STA 449 F3 Jupiter), from room temperature (RT) to 550 ºC with a heating rate of 5 ºCmin^{-1}, in an aluminum pan, under air atmosphere.

3.1.5. Screen-printing of conductive patterns

3.1.5.1. Surface properties and thermal stability analysis of different paper substrates

Three different types of paper substrates were initially considered in order to print the formulated inks: two distinct photographic papers produced by Felix Schoeller (referred to as paper FS2 and FS3) and commercially available printing paper (300 % from Soporcel).Their surface topography and cross section was analyzed by SEM, and three-dimensional (3D) profilometry of surface was performed with an Ambios XP-Plus 200 Stylus Profilometer and the software data compilation from TrueMap. Contact angle measurements of the solvents used in the inks formulation, such as water and a mixture of toluene:ethanol (80:20 % v/v) on the surface of paper were performed using a Dataphysics OCA-15plus Syste, using a 2 µl liquid drop and at least 3 readings were taken on each sample, for different times. The thermal stability was studied by TGA using the same setup and measurement conditions described in 3.1.4.2.

3.1.5.2. Deposition of conductive patterns

The deposition of cellulose-based conductive composite inks was carried out on paper FS3. Because of the relatively high length of the CFs, a patterned polyester screen mold was designed and ordered in a local polygraphic company (I.C.M. Graf, Portugal) with the following characteristics: mesh model, 77-55; mesh count, 190 mesh/inch; aperture, 81 µm; thread diameter, 55 µm; opening, 30 %; fabric thickness, 88-97 µm. Several samples were prepared in order to understand the influence of the number of printing passes (from 1 to 10) and drying conditions performed between each printing pass on their print quality and electrical performance. Each printed layer was dried either at RT conditions for 15 min or in an oven at 120 ºC for 15 min. The latter one was only applied for the electroconductive printed films based on CMC.

In the case of MWCNTs used as electroconductive material, since the particle dimensions do not impose physical limitations to the mesh dimensions, screen printing was carried out using an additional screen mold with following characteristics: mesh model, 120-34; mesh count, 305 mesh/inch; aperture, 45 µm; thread diameter, 34 µm; opening, 30.5%; fabric thickness, 52-57 µm. In order to study the resistivity thickness dependence, several printing passes were performed (from 1 to 10) and each layer was dried at RT for 15 min.

3.1.5.3. Characterization of conductive patterns

To investigate the continuity and uniformity of the printed patterns, an optical microscope was used. The thickness was estimated by optical micrographs of the cross-section of printed patterns. The resistivity of the printed patterns was measured using a four-point probe resistivity measurement system (Jandel Engineering). Because resistivity of printed patterns is highly dependent of atmospheric conditions, a glove box with controlled temperature (21-24 ºC) and humidity (13-15 % RH) conditions was also used to perform electrical measurements. To evaluate the flexibility of the printed films and predict behavior under stressing mechanical condition, they were subjected to deformation through bending cycles (1-1000 cycles) and under several folding radius (0-180 º), in both sides of the samples. Fourrier transform infrared spectroscopy analysis was used to evaluate the solvent evaporation from samples and spectra was acquired within in a range of 4500-525 cm^{-1} with 2 cm^{-1} step using an attenuated total reflectance (ATR) sampling accessory (Smart iTR) equipped with a single-bounce diamond crystal on a Thermo Nicolet 6700 Spectrometer.

3.2. Cellulose-based hydrogels applied as the gate dielectric in electrolyte-gated transistors for printed electronics

3.2.1. Materials and methods

All reagents were used without further purification. MCC (powder, 20 μm), LiOH (≥ 98) and acetic acid (≥ 99 %) were purchased from Sigma-Aldrich. Urea (≥ 99.5 %) was purchased from Carl Roth, ethanol analytical reagent grade was provided by Fisher Scientific and toluene (≥ 99%) was purchased from Merck. Deionized water (Millipore) was used.

3.2.2. Preparation and characterization of cellulose-based hydrogels electrolytes

3.1.2.1. Preparation of cellulose-based hydrogels electrolytes

An aqueous solution of LiOH/urea with the optimal mass ratio of 4.6:15 wt%, as reported in the literature [9], was used as solvent system in this study. The solution was then pre-cooled in a freezer at -25 ºC, until complete solidification. The frozen solution was then allowed to thaw at RT and the desired amount of MCC was dispersed in the precooled solvent under vigorous stirring at -8 ºC, until its complete dissolution. Additionally, the mixture was neutralized with acetic acid, in order not to damage other layers existing in the final device, and simultaneously cellulose was regenerated. The solutions were stored in a refrigerator at 3 ºC, until being used. Annex H summarizes the electrolyte solutions prepared and the nomenclature attributed to each one, considering their weight percentage.

Electrolyte membranes were prepared for characterization by slow casting and evaporation of water from 10 g of solution under ambient conditions in polystyrene Petri dishes (5.5 cm diameter). The thickness of the resulting membranes was estimated from the average of five measurements using a Mitutoyo digital micrometer.

3.1.2.2. Characterization of cellulose-based hydrogels electrolytes

Electrochemical characterization of the electrolytes was carried at RT, in a typical capacitor structure by depositing the electrolyte between two stainless steel discs with an active area of 0.994 cm^2, using a Gamry Instruments Reference 600 potentiostat. Electrochemical impedance spectroscopy (EIS) measurements were performed at 1 V with a superimposed 5 mV AC voltage in a frequency range of 10^5 Hz to 0.1 Hz. Cyclic voltammetry (CV) measurements were performed in a potential range between -2 V and 2 V, using different scan rates from 25 to 100 mV/s.

3.2.3. Fabrication and characterization of electrolyte-gated transistors

The EGTs devices were produced by conventional physical vapor deposition (PVD), and cellulose-based electrolytes as the gate dielectric. A planar configuration was adopted, using titanium/gold (Ti/Au) as bottom electrodes (source, drain and gate) deposited on glass (Marienfeld) in a conventional architecture, followed by GIZO working as the active oxide semiconductor.

One initial concern of the fabrication process is the substrate cleaning carried out in an ultrasonic bath for 10 minutes, first in acetone and then in isopropanol, after that, rinsed off in deionized water and dried using nitrogen. Afterwards, Ti/Au electrical contacts (6 and 65 nm thick, respectively) were deposited by e-beam evaporation. Then a 35 nm GIZO (Ga_2O_3–In_2O_3–ZnO; 1:2:2 mol %) layer was deposited over the patterned electrical contacts region by radio-frequency (RF) magnetron sputtering, at RT, in an AJA ORION system. The semiconductor channel and the electrical patterns were patterned with shadow masks with a channel width (W) of 950 μm and length (L) of 190 μm (W/L = 5). A schematic representation of the proposed devices and fabrication steps and layers with corresponding thickness is given on Annex I.

The EGTs were electrically analyzed in the dark at room temperature using a microprobe station Cascade Microtech M150) connected to a semiconductor parameter analyzer (Agilent 4155C) controlled by the software Metrics ICS. The top contact of the printed EGTs devices was obtained using the tip of the equipment.

4. RESULTS AND DISCUSSION

4.1. Printable cellulose-based electroconductive composite film for paper electronics

4.1.1. Structural, morphological and electrical characterization of carbon fibers

Figure 4.1 a) shows a picture of pristine CFs which exhibit a cylindrical shape with a diameter around 7 µm and a length size around 150 µm, as shown in Figure 4.1b)-c). A high aspect ratio (length/diameter) of the fibers is desirable to improve electrical performance, however CFs with such long length can be a problem for printing. Due to the relatively high length size of the provided CFs, which is slightly bigger than the aperture of the used screen (81 µm) most of the fibers are not able to pass through the screen, affecting the printed pattern and final electrical performance.

In an attempt to reduce their length size, grinding and ultrasonication were performed. Comparing milled (Figure 4.1 d) with sonicated CFs (Figure 4.1 e), it's clear that the former can significantly alter the morphology of CFs, being severely damage in some cases, reducing the fibers length. On the other hand, sonicated CFs exhibits a morphology very similar to as received pristine CFs. In order to get a better understanding of the influence of each mechanical treatment in the length distribution of CFs, a simple statistical study was carried out by comparing optical microscope images with 200 individual fibers and estimate their length size with ImageJ software.

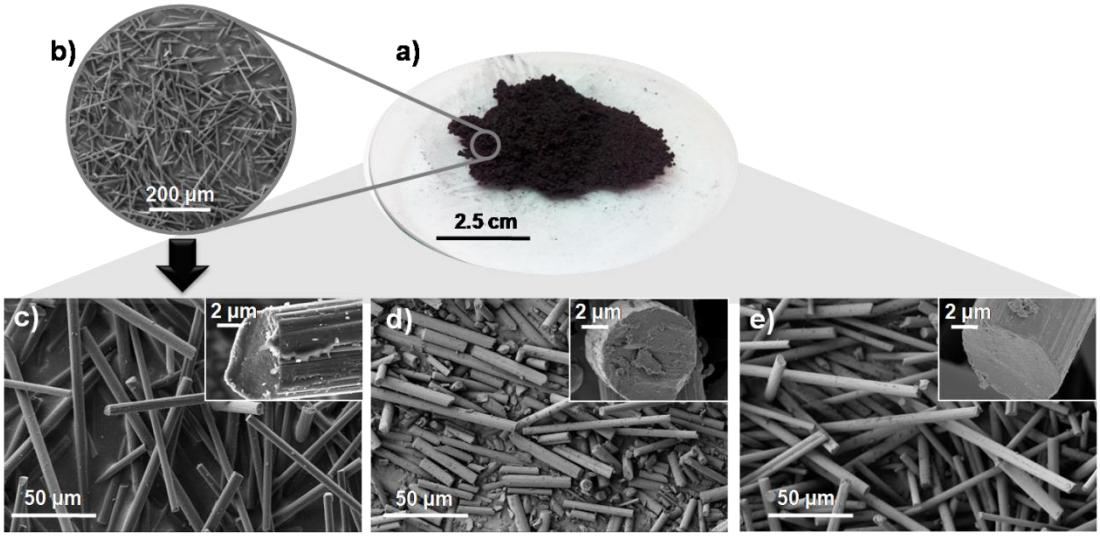

Figure 4.1 - Photograph of pristine CFs (a) and respective SEM images (b,c). SEM images of CFs after milling (d) and 6h of ultrasonication (e).

As represented in Figure 4.2 a, pristine CFs shows a wide length distribution with an average length size of 123 µm and a standard deviation of 79 µm. More than 60 % of the fibers have a length higher than 81 µm (mesh opening).

For sonicated CFs, samples were collected after 30, 60, 120 and 360 minutes of ultrasonication. In Figure 4.2 is represented the percentage of fibers whose length is higher than 80 µm for different sonication times. For as received pristine CFs, only 45.7 % of the population seem to have a length smaller than 100 µm increasing to 63.4 % after 120 minutes. Longer periods of time seem to not affect significantly this percentage, since that for 360 minutes of sonication, it increases less than 2 %. After milling of the CFs, another sample was observed on optical microscope and again 200 randomly selected fibers were subjected to statistical analysis. In Figure 4.2c), the distribution of the fibers reveals significant differences since 92.5 % seem to have less than 81 µm of length. Thus, milling reveled to be a much more effective treatment than sonication for decreasing fibers length.

According to these results, only pristine and milled CFs were used in the formulation of conductive inks for comparison of the electrical performance. No further study was performed on sonicated CFs.

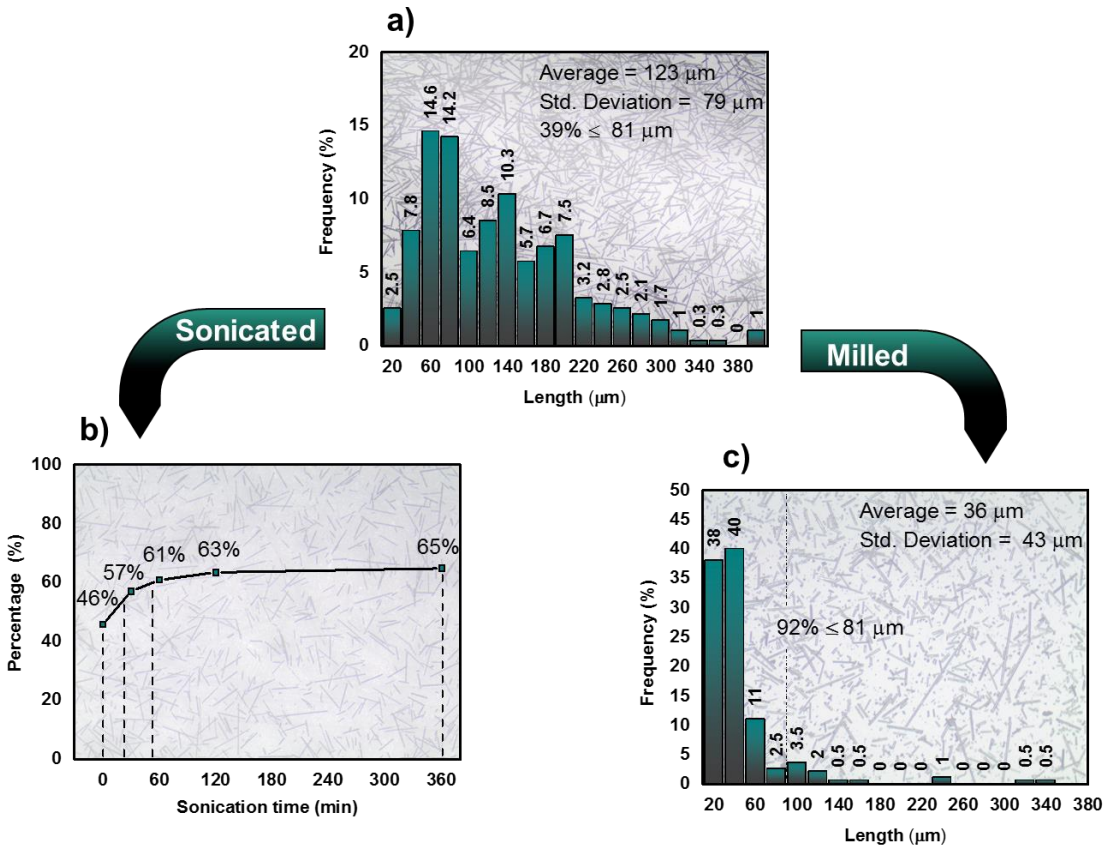

Figure 4.2 - Statistical study perfomed on CFs in order to optimize their length size (a) by ultrasonication (the graph shows the percentage of fibers with lengths lower than 81 µm) (b) and milling (c).

The XRD patterns of CFs (pristine, milled and sonicated) are shown in Figure 4.3 a), where the characteristic peaks of hexagonal carbon phase (ICDD File: 00-041-1487) can be identified.[77] All samples reveal one predominant peak at 25.0 º corresponding to (002) plane and two broad peaks less intense around 43.9 º and 51.8 º associated, respectively, to (101) and (004) crystallographic planes.

Regarding in situ XRD measurements performed to pristine CFs under different temperatures from RT to 500 ºC (Figure 4.3b), it is possible to conclude that their structure is not affected, exhibiting thermal stability in this range of temperatures.

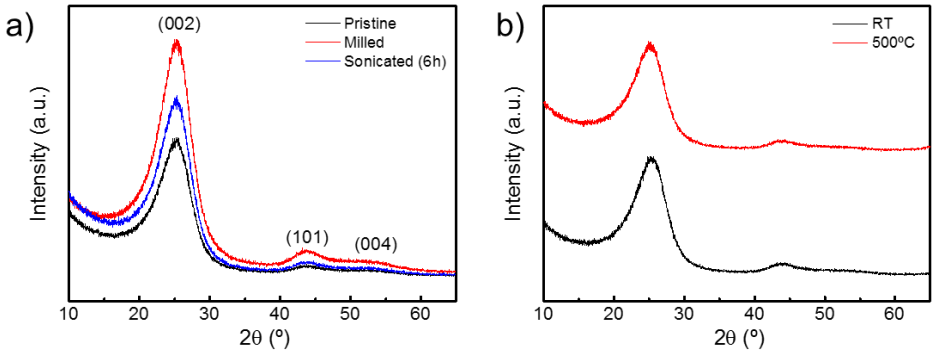

Figure 4.3 - Structural characterization of CFs (pristine, milled and sonicated) by XRD (a) and influence of temperature on pristine CFs structure (b).

Electrical characterization of CFs was performed in order to find the resistivity of individual fibers and to quantify the effect of contact resistance between them in electrical conduction. Due to the small size of the fibers, which are difficult to handle, carbon ribbons precursors of CFs were used instead. Silver paste was used to improve the connection between the ribbons and the probes. Figure 4.4 b) and c) shows the assembly used to quantify the contact resistance between carbon ribbons, being the resistance of one single ribbon compared with the resistance of two ribbons attached to each other.

Electrical resistance of an individual carbon ribbon with a length size of 10.4 cm was measured with a multimeter as 35.3 kΩ. Using expression on Annex J and knowing that ribbon diameter is 7 µm, the resistivity was estimated around 1.30×10^{-3} Ωcm. Several measurements of two carbon ribbons connected at some point with a resultant different length was also measured and the linear regression of the collected data is shown in Figure 4.4 a).The slope value (3.43 $k\Omega cm^{-1}$) from linear regression represents the resistance per length unit of the ribbons and the correspondent resistivity (1.32×10^{3} Ωcm), calculated from equation 1, reveals a very similar value for the single fiber with a relative error of 1.54 %. The interception with Y axis is the contribution of contact resistance of the ribbon connection and its value is 0.91 kΩ, which is a significant contribution to the final resistance of the material.

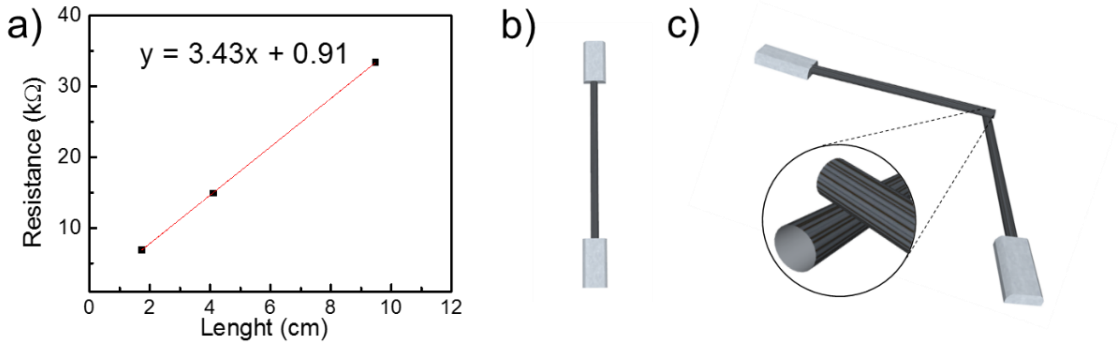

Figure 4.4–a) Linear regression of resistance values of several carbon ribbons with different lenghts; representation of the assembly used to measure resistance from a single carbon ribbon (b) and from two carbon ribbons with a connection point (c).

4.1.2. Structural and morphological characterization of multi-walled carbon nanotubes

Figure 4.5 a) shows SEM images of MWCNTs that were previously dispersed in aqueous solution with a few drops of Triton-X100 and then subjected to ultrasonication for 30 min. This preparation method described in literature [78] was performed in order to improve the dispersion of MWCNTs for SEM imaging, since they are not functionalized and have the tendency to form clusters promoted by Van der Walls attraction [23]. Wherein, it is possible to distinguish individual MWCNTs with length sizes from 1 to 4.3 µm and a diameter of about 15 nm.

XRD analysis of MWCNTs, represented in Figure 4.5 b), shows characteristic peaks at 25.56 º (002), 34.21 º (111) and 43.69 º (101). The XRD pattern of graphite can be used for interpretation with some margin of error since MWCNTs do not present a 3D structure. [79] Wherein, 25.56 º and 43.69 º peak are characteristic of hexagonal graphite (ICDD File: 00-041-1487) and peak at 34.21 º is intended to be associated to some oxidation of the carbon structures (ICDD File: 00-047-1071). The latter peak is related to the presence of CO_2 in the atmosphere, during the measurements. However, the analysis of MWCNTs patterns is not straight forward, since their size, curvature and stacking of graphene layers can lead to peak shifts and broadenings. [79]

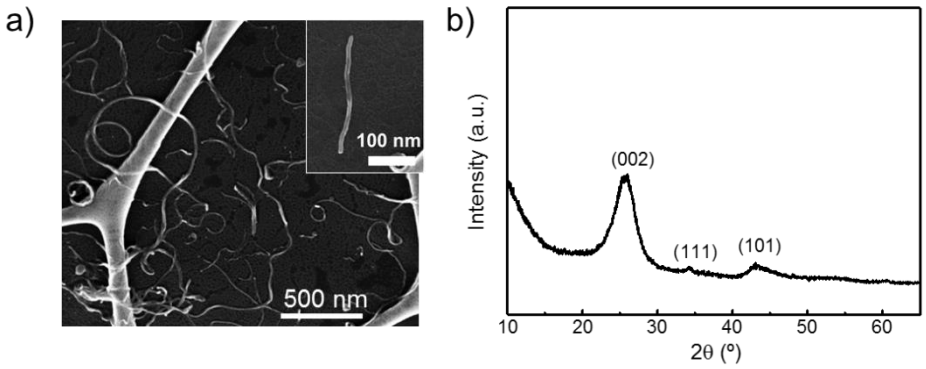

Figure 4.5 –SEM images(a) and XRD diffractogram of MWCNTs (b).

4.1.3. Surface properties and thermal stability analysis of different paper substrates

In order to get a functional printed layer with a good printing resolution, there are some concerns related with the ink rheological properties, which must be adapted to each type of substrate used. Wettability and surface morphology are some important parameters that must be considered for selection of a substrate for printed electronics. Furthermore, sometimes is required an additional step of annealing at high temperature for improvement of required properties of the functional printed layer, by removal of solvent trapped in a wet printed layer or elimination of the sacrificial binder. Thus, substrate should be thermodynamically stable under a certain range of temperatures. In this work, three cellulose-based substrates were studied: regular printing paper, paper FS2 and paper FS3.

SEM image of conventional printing paper is shown on a), and its surface reveals a matrix of randomly dispersed long cellulose fibers of about 5 to 15 µm width. Fibers also seem to be flattened, probably due to the compression (calendaring) step during the manufacturing process. Cross section shows packed fibers with a similar structure along paper thickness.

Papers FS2 and FS3 exhibit a much smoother and nanoporous surface as shown on Figure 4.6 b) and c), respectively, contrasting with conventional printing paper. From cross section images it is possible to distinguish different coating layers on the top and bottom side of the raw paper and their respective dimensions. Both papers show one bottom and two top coatings, being the latter responsible for the nanoporous surface. According to the specifications provided by the manufacture, paper FS2 consists of a thick raw paper with a thin backcoating layer, with a pre-coat and nanoporous coating on the top side. For paper FS3, the backcoat and pre-coat are replaced by a resin coating.

The thickness values of each substrate are indicated in Table 4.1. Paper FS2 is thicker than paper FS3, and regular paper is the thinnest from the three substrates.

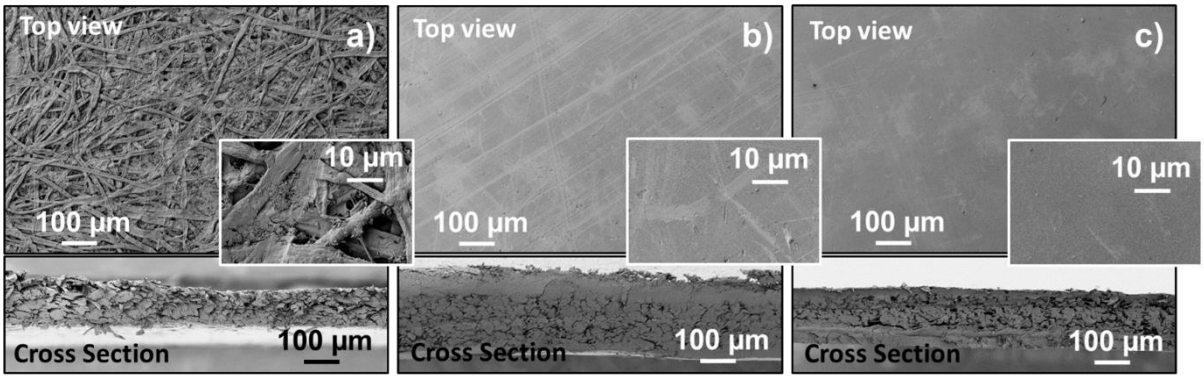

Figure 4.6–SEM images top view and cross section of a) regular printing paper, b) paper FS2 and c) paper FS3.

Table 4.1–Thickness measurements of the three types of paper.

	Regular Paper	FS2	FS3
Thickness (µm)	107.40	207.80	180.80

Although through SEM analysis is possible to get some information about surface morphology, 3D scanning profilometry can provide some extra information about the paper surface roughness and quantify it.

Figure 4.7 represents the results of the 3D scans performed on the substrate surfaces along an area of (0.5x0.5) mm^2. Regular printing paper (Figure 4.7 a) have a peak to valley height of 19.71 µm and a root mean square (RMS) roughness of 2.99 µm, while papers FS2 (Figure 4.7 b) and FS3 (Figure 4.7c) have a peak to valley height of 2.38 and 1.38 µm respectively, and a RMS roughness of 283 and 251 nm. Regular paper surface is extremely irregular, when compared to papers FS2 and FS3, which have a very smooth surface roughness. Comparing the three papers, paper FS3 exhibits the smoothest surface.

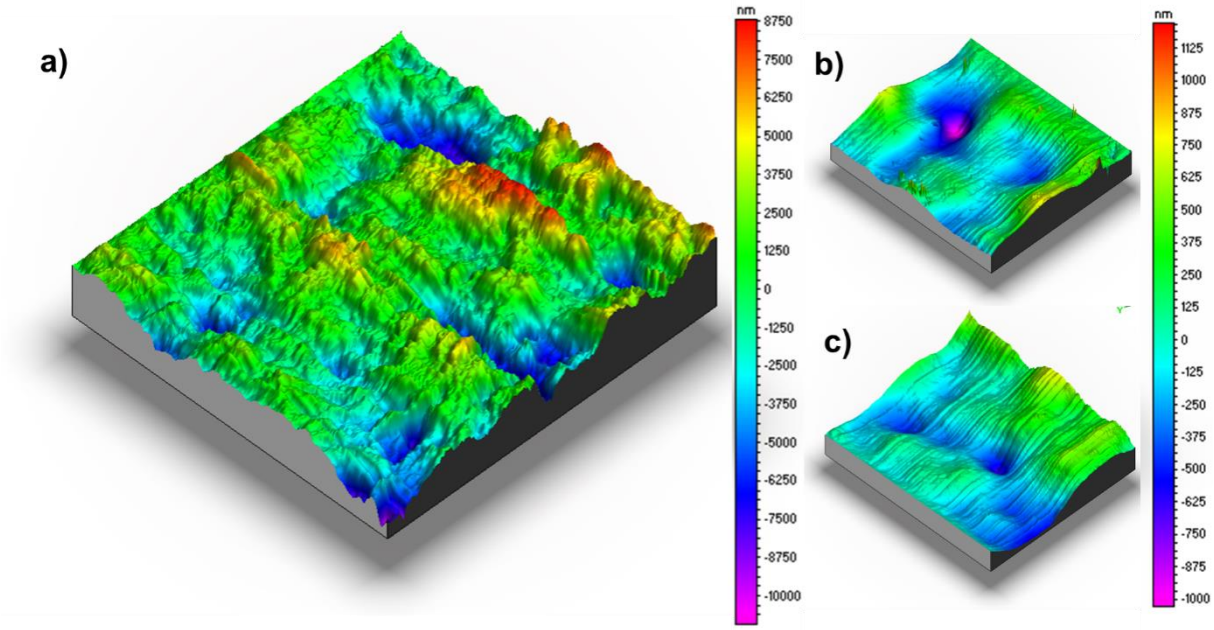

Figure 4.7 – Topographic mapping of regular printing paper (a), paper FS2 (b) and paper FS3 (c) through 3D profilometry on an area of 0.5x0.5 mm^2.

Sessile drop method was performed on the paper substrates testing the solvents used in the formulation of the inks, such as water and a mixture of toluene and ethanol (80:20 % v/v), in order to determine their contact angle. The results are illustrated in Figure 4.8 a)-c), which were obtained right after the droplet has reached the substrate surface.

Regular printing paper reveals a hydrophobic behavior for the water droplet, with a contact angle of 100.8 ºC (Figure 4.8 a) at the moment right after being dropped on the surface however, it takes only a few seconds for the water drop being absorbed by the porous structure of paper, while Toluene/ethanol mixture is immediately absorbed. On the other hand, surface properties of FS2 and FS3 papers are quite different when compared with regular paper. In a general manner, these papers exhibit a hydrophilic behavior, either in contact with water or a mixture of ethanol and toluene. Paper FS2 is more hydrophilic than paper FS3, with a contact angle of 27.2 º against 73.2 º, when in contact with water (Figure 4.8 b) and c). Both papers are highly hydrophilic for the organic solvent mixture, with contact angles below to 10 º (Figure 4.8 d) and e). It's important to notice that the nanoporous top layer of FS2 and FS3 papers is resistant to the solvents used in the composition of the inks, preventing their absorption through the substrate. Both substrates are suitable for printed electronics, being possible to host an electronic device on their surface.

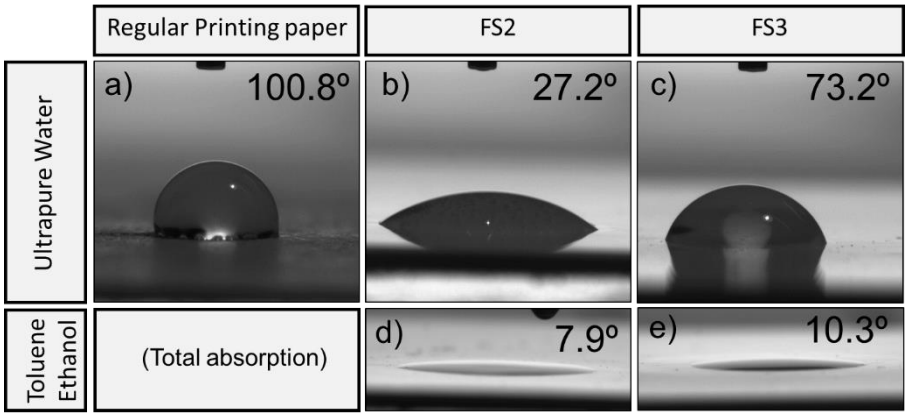

Figure 4.8– Contact angle measured with sessile drop method with a volume of 2 µL of ultrapure water on regular printing paper (a), FS2 paper (b), FS3 paper (c) and 2 µL of a solution of toluene/ethanol (80:20) on FS2 paper (d) and FS3 paper (e).

Additionally to these studies, it was also analyzed the influence of the temperature on the degradation of the paper substrates by TGA analysis from RT up to 500 ºC. From Figure 4.9 it's possible

to see a similar loss of mass on all the substrates below 100 ºC, which is related to the loss of water that is adsorbed on their surface. Moreover, it's clear that the fibrous and porous structure of the regular printing paper allows the trapping of a bigger amount of water on its structure, as shown in Figure 4.9 a). All the substrates are stable up to 200 ºC, occurring an abrupt loss of mass for as the temperature increases up to 350 ºC, with similar mass loss percentage for FS2 and FS3 papers (42.55 and 40.17 percentage points (pp), respectively) and a larger percentage for regular printing paper (53.86 %). Since cellulose is the common material of all the substrates, this sudden loss of mass is associated to its degradation [80][81][82].

It is important to correlate these results with the drying conditions chosen for each printed layer of the screen-printed patterns, which are studied in more detailed in 4.1.4. TGA results demonstrate that temperatures below 200 ºC are suitable for drying each printed layer without damaging the paper substrate.

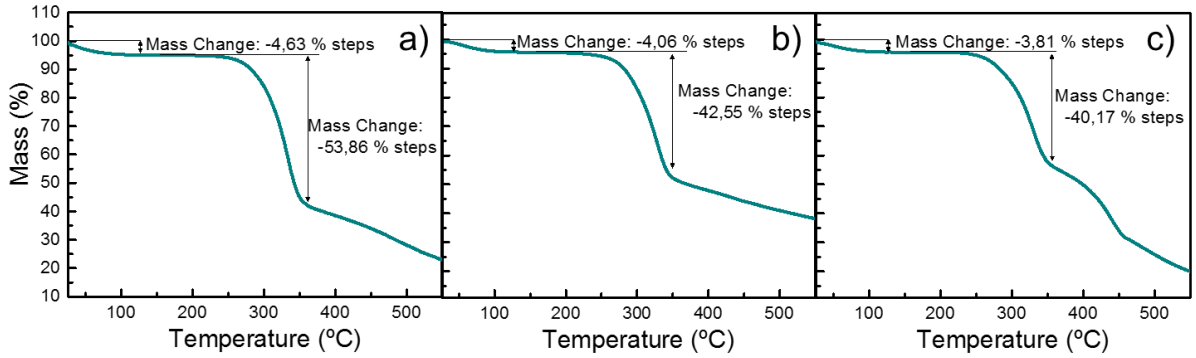

Figure 4.9–Thermogravimetric analysis for regular printing paper (a), FS2 (b) and FS3 (c).

Taking into consideration the surface properties of the substrates and their thermal stability, one of them was selected as substrate for screen-printing of the developed inks. From the correlation of SEM, contact angles and TGA results, it is possible to conclude that paper FS3 is the more advantageous substrate among the three studied substrates, as shown in Table 4.2, presenting the following characteristics:

- Smooth and impermeable surface conferred by a polymeric nanoporous coating;
- Hydrophilic surface, either in contact with water or a mixture of toluene and ethanol;
- Thermal stability until 200 ºC.

Table 4.2–Summary of relative advantages of different paper substrates for printed electronics,according to the characterization results.

	SEM	3D Profilometry	Contact angle	TGA
Regular printing paper	🟡	🔴	🔴	🟢
FS2	🟢	🟡	🟡	🟢
FS3	🟢	🟢	🟢	🟢

4.1.4. Characterization of formulated screen-printing inks and quality of printed patterns

The use of screen-printing technique to the deposition of electroconductive functional materials demands the formulation of suitable inks. It's important to find the best combination between each component, in order to provide optimal printing performance combined with high electrical conductivity.

Preparation of such inks is challenging, due to the high viscosity required, which can be achieved through the addition of polymer binders (like cellulose derivatives, for instance), to the ink composition. Additionally, there are some concerns related to the development of MWCNTs and CFs-based electroconductive inks because, due to their hydrophobicity and large aspect ratio, van der Waals forces promote the formation of large bundles or ropes. Several approaches are reported in order to obtain a stable dispersion of the carbon structures through their dispersion in organic solvents without

dispersing agents, in aqueous media using surfactants or polymers, or through their modification with functional groups, favoring their interactions with the dispersing medium [24]. The use of cellulose derivatives as dispersants of carbon structures was already demonstrated. [25][26] It is important to mention that CMC is water soluble and has been successfully used as excellent dispersant for single-walled CNTs, presenting a good film-forming ability [26] and also as suitable thickener agent in screen printing inks. [83] Also, EC is soluble on organic solvent and is very commonly used in the formulation of screen printing inks. [44][46][86][87]

In this work, cellulose-based electroconductive composite inks for screen-printing were formulated, using a simple and eco-friendly method by blending either CFs or MWCNTs into the matrix of a cellulose derivative (CMC or EC).

4.1.4.1. Optimization of binder content to enhance print quality of the electroconductive inks

For the printing of the electroconductive composites, it is fundamental to find the minimum amount of binder to achieve the best printing resolution of the printed films. Several solutions were prepared using different concentrations of cellulose derivative (CMC or EC) from 2 to 5% wt., without adding the conductive functional material. These solutions were screen printed using a patterned resolution test lines with different widths, as shown in Annex K, being the width of the lines the same as the space between them. The printed patterns were observed with an optical microscope and a photograph was taken when EC and CMC solutions, with concentrations from 2 to 5% wt. (Figure 4.10 a- h).

EC solutions with a concentration below 4 % wt. are not suitable for screen printing, since the viscosity is too low, leading to merged lines and an undefined pattern. Although, it is possible to print a defined line pattern using a solution of EC with a concentration of 4 % wt., the resolution is still not good. The best printed line was obtained for a concentration of 5 % wt., result in printed lines width of 362 µm, using a line pattern of 275 µm. On the other hand, it was noticed that is possible to obtain printed patterns with line width of 275 µm width even for lower concentrations of CMC (2 % wt.). However, for the solution with 2 % wt. of CMC viscosity is too low and it drains tough mesh openings even without squeegee being applied. The same does not happen if increasing the binder proportion to 3 % wt. of CMC, in which a resolution of about 345 µm is achieved (see Annex L).

From this study, it was demonstrated that both EC and CMC solutions in proportions of 5 % and 3 % wt., respectively, are suitable for screen printing. For that reason, both cellulose derivatives were used as binders to fabricate electroconductive screen printing inks and its electrical performance is compared on sub-section 4.1.6.

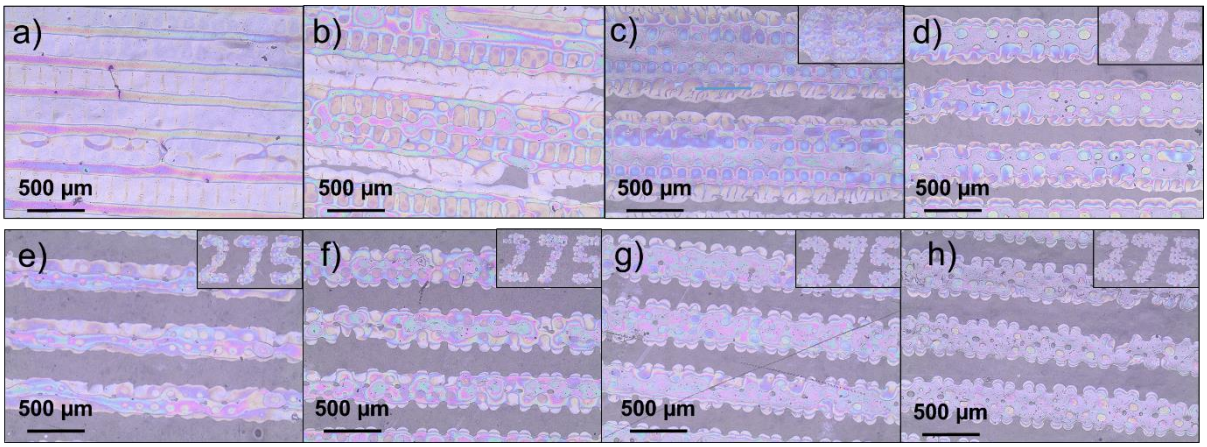

Figure 4.10–Optical micoscope images of the narrower and continuous screen printed lines (on the top at the right) obtaind for EC solution with proportions from 2 to 5 %wt (a-d) and CMC solutions proportions from 2 to 5 % wt. (e-h).

Although, the use of binders is essential in order to improve the ink stability and printability, their presence is at the same time problematic, since they are non-conducting materials. Thus, their existence between the particles will have a negative influence on the electrical performance. Therefore, a balance between the content of carbon material and cellulose binder should be found in order to obtain a

conductive printed layer, where direct electrical contacts between the conducting carbon structures in the printed pattern is critical.

Since such inks are aimed to result in conductive printed patterns, it is essential that the concentration of the conductive functional material is high. For this reason, CFs- and MWCNTs-based inks were prepared changing the content of the respective carbon material, from 5 to 10 % wt., in the former case, and from 0.1 to 0.5 % wt., in the latter case. As it was mentioned before in sub-section 4.1.1, milled CFs were selected for the formulation of the inks and compared with those prepared with pristine CFs, although the latter ones exhibit a high length dispersion, being most part of them bigger than the mesh opening (81 µm) of the screen mold.

4.1.4.2. Physical properties of the formulated electroconductive inks

When it comes to screen printing, shear rate can be interpreted as a combination of factors, like pressure and velocity applied to squeegee and screen tension. Inks are subjected to different amount of shear stress through the printing process, and so it is important to know their rheological properties. In order to study them, the inks were subjected to viscosity measurement under controlled shear rates from 10^{-1} to 10^{3} s^{-1}. The results are resumed on Figure 4.11. The main contribution for the rheological behavior of the inks is given by the cellulose binders used in their composition, although the addition of functional materials also affects it. Figure 4.11 shows that both EC and CMC-based electroconductive inks have a non-Newtonian behavior, since viscosity is a function of applied shear rate. All inks have in common that viscosity decreases with applied shear rate (shear thinning behavior), and for that reason they can be classified as pseudo-plastic.

During the first stage of the screen printing process, a high viscosity is required to maintain the ink on the mesh. Then, a low viscosity is desirable to easily transfer the ink through the mesh holes onto the substrate, during the squeezing step. Finally, after printing, the high viscosity recovery should take a short period of time, to allow the ink to level and became uniformly spread in the substrate. Since the developed inks have a shear thinning behavior, this feature makes these inks suitable for screen printing.

In literature, typical values for screen printing inks are not very consensual are vary in the range from 1-300 Pas [35][84]. Also, inks for better line resolution usually have higher viscosity values. [84][85] Comparing the inks based on CFs, formulated EC- and CMC-based inks exhibit viscosities under the range of 14.78 – 71.23 and 4.32 – 7.48 Pas, respectively, for a shear rate of 10^{1} s^{-1}. In a general manner, the addition of solid components to the binder solutions increases the viscosity of the inks, being the viscosity higher for pristine CFs, which exhibit a longer length size when compared to milled CFs. Considering these values, the formulated inks are suitable for screen printing.

Also, it is expected that EC-based inks show the best resolution of printing patterns, due to their higher viscosity. In particular, EC5 CF10 ink has the highest viscosity for low shear rates and the lowest viscosity for high shear rates, which makes it by principle the best ink to be printed, though there is not guarantee that such large shear rate would ever be achieved in screen printing. [86]. However, as it'll be mentioned in sub-section 4.1.4.4., CMC-based inks have a better printing resolution reaching width lines of 400 µm, against 480 µm obtained for EC-based using the same pattern. This occurrence is possibly related to the thixotropy of the inks. After a shear rate being applied to a fluid, it takes a certain amount of time to recover its steady properties. If that recovery time is too long, the printed ink can spreads through the substrate surface and reduce the printing resolution, resulting in thicker lines. [87][44] However, this theory is not possible to be confirmed with the existing data.

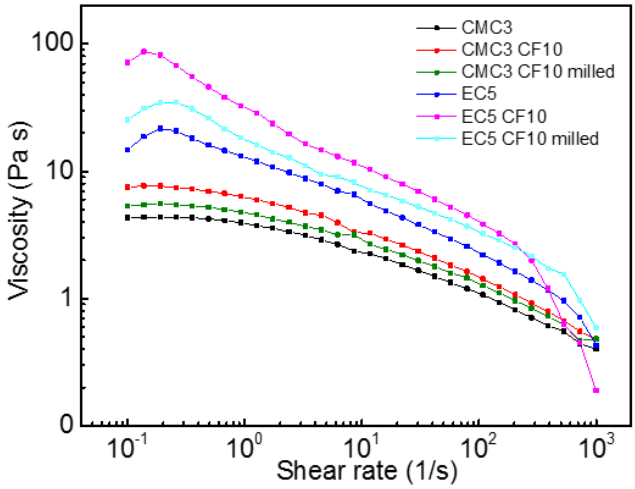

Figure 4.11–Dinamic viscosity of CMC and EC based inks under shear rates from 0.1 to 1000 s^{-1}.

TGA analysis of formulated inks was performed in order to study it's degradation with temperature. Figure 4.12 a) and c) shows the data of CMC-based electroconductive inks, using either pristine CFs (10 % wt.) or MWCNTs (0.5 % wt.) as conductive functional material. For the two CMC based inks, the first significant loss of mass occurs below 100 ºC and is related to water evaporation. In both cases, it's observed a second mass loss between 250 and 325 ºC, related to degradation of CMC [88]. Due to the high volatility of the solvents in the EC-based inks and some initial evaporation, the weight loss measured from TGA doesn't correspond to its real mass content. However, it is still possible to identify relevant mass losses (see Figure 4.12 b) and d) below 120 ºC associated to remaining solvents' evaporation (toluene and ethanol). The second mass loss situates in the range between 225 and 350 ºC and is related to EC degradation, as suggested in the literature [89]. In conclusion, CMC and EC-based inks are thermally stable under 250 and 225 ºC, respectively. According to that and, since water, ethanol and toluene have boiling points below 120 ºC (100, 78 and 110 ºC, respectively) the influence of drying conditions on the print quality and electrical performance of the printed patterns was studied. (See sub-section 4.1.4.3.).

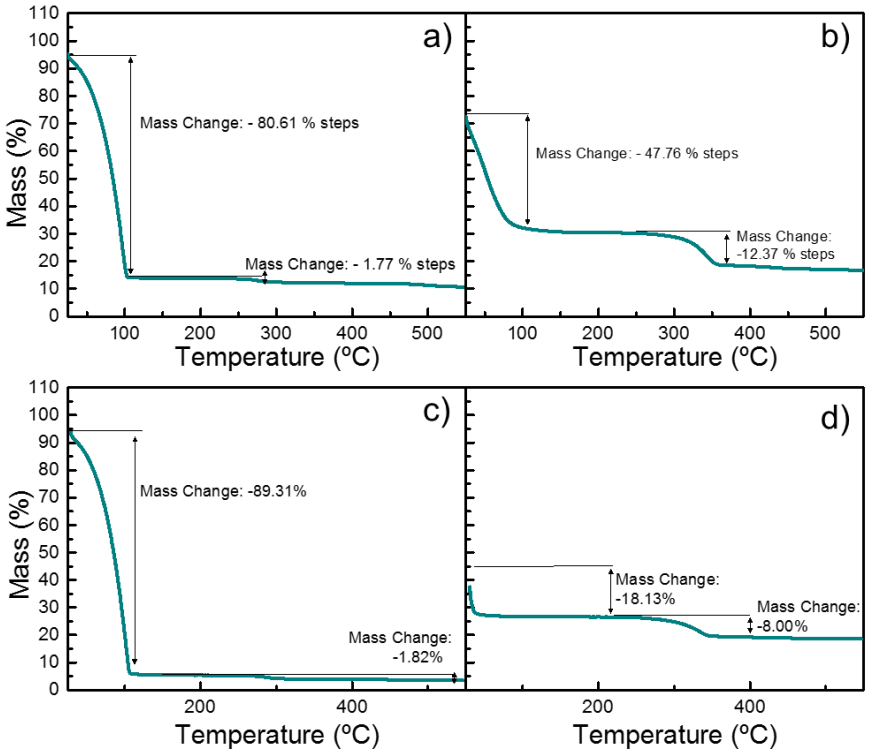

Figure 4.12 – TGA analysis of CMC3CF10 (a), EC5 CF10 (b), CMC3 CNT0.5 (c) and EC5 CNT0.5 (d) inks.

4.1.4.3. Optimization of drying conditions to enhance print quality of the electroconductive inks

The drying conditions affect water retention in the printed films and their ability to partially dissolve the surface of each printed layer obtained through different printing passes, having influence on the electrical performance and the print quality. Additionally, drying temperature was limited to 120 ºC, respecting the temperature tolerance of paper FS3 used as substrate and thermal stability of the formulated inks, as it was mentioned before.

FTIR analysis was performed right after screen printing of CMC3 and EC5 solutions and after drying for different times, from 5 to 30 minutes, either at RT or in an oven at 120 ºC, in air at atmospheric pressure. The results of EC printed layer dried at different conditions are shown on Figure 4.13a). It's possible to identify vibrational stretching modes of -OH (3475 cm^{-1}) related to intra and intermolecular bonds in the ring structure, -CH (related to the neighboring peaks in the region between 2973 and 2869 cm^{-1}),-CH_2 (1454 cm^{-1}), -CH_3 (1375 cm^{-1}), C-O-C (1066 cm^{-1}), in good agreement with EC characteristic spectra obtained in literature. [90] The –OH peak (3475 cm^{-1}) is probably also associated to the presence of ethanol in the film and the presence of toluene is confirmed by the C=C associated peak (1442 cm^{-1}) [91].

A closer look in the evolution of the relative intensity of these peaks can provide a good description of the influence of temperature and time on evaporation of these solvents (detail in Figure 4.13 a). In general, longer drying times promote evaporation of the solvents, and higher temperatures speed up the process, as it is demonstrated by the decrease of the peaks' intensity. After drying at RT for 5 min, the relative intensity of ethanol and toluene peaks have no significant change, being slightly less intense for the sample dried at 120 ºC. The intensity of these characteristic peaks keep decreasing with drying time, from 15 to 30 min, but there are no significant differences between RT and 120 ºC. After 30 min, there's again a significant decrease in peaks intensity for both temperatures. In conclusion, it is needed a minimum drying time of 15 and 5 min for RT and 120 ºC, respectively, to promote evaporation of the solvents.

From FTIR spectra obtained for CMC printed films (Figure 4.13b), it's possible to identify, among others, vibrational stretching modes of -CH_2 and -OH (2917 and 1415 cm^{-1}) from the methane ring and -C=O characteristic of COOH from carboxyl groups of CMC (1587 cm^{-1}). [92][93] It was expected that the peak associated to –OH group (from water adsorbed in the structure) to be centered at 3500 cm^{-1}, instead of 3261 cm^{-1}. Nevertheless this similar peak position was observed when analyzing ultrapure water (Annex M). So, a closer look to this peak can also provide information about the effectiveness of the drying conditions. Detail in Figure 4.13b shows a slight decrease in peak intensity after only 5 min of at RT, keep decreasing with drying time. Nevertheless, the reduction of the peak intensity is more evident for 120 ºC, not changing significantly for longer periods. On the other hand, the samples dried at RT need at least 30 min to achieve a similar and notorious water loss. According to these results, in order to study the influence of the drying conditions on the electrical performance of the carbon-based printed films (sub-section 4.1.5.3.), the following conditions were selected for further study:

- For CMC-based inks: RT for 15 min and 120 ºC for 15 min.
- For EC-based inks: RT for 15 min.

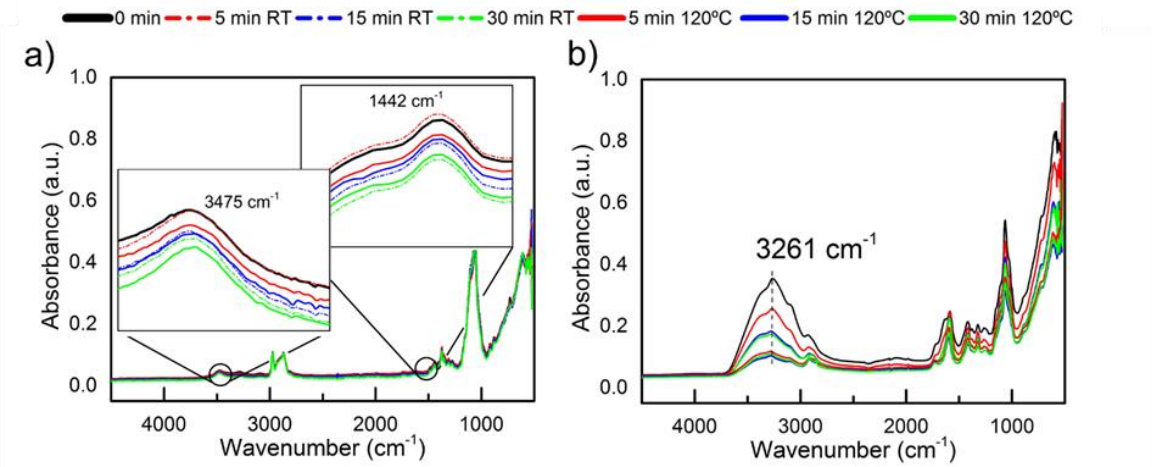

Figure 4.13 – FTIR spectra of EC5 (a) and CMC3 (b) solutions measuredt after, 5, 15 30 min after screen printing.

4.1.4.4. Influence of carbon materials content on print quality of the electroconductive inks

In Figure 4.14 is shown the print quality of single printed layers of the conductive inks, which were dried at RT. This results are correlated with the content of the carbon material, cellulose derivative (used as dispersing and stabilizing agent) and drying conditions, which have a great influence on the printing quality of the films. Since the drying conditions revealed not to have a significant impact on electrical performance, as demonstrated by Figure 4.21, this parameter was not studied extensively in this sub-section. However, the drying conditions have influence on the electrical performance, due to the water retention in the films, as it will be explained in sub-section 4.1.5. Regarding CF content, it is clear that one printing pass is not enough to ensure an efficient contact between the printed fibers, even for the highest CFs concentration (10 % wt.), and independently of the cellulose binder used and morphology adopted for the CFs (pristine or milled). For this reason, the effect of the number of printing passes was also studied, in order to correlate the dependence of film thickness with the final electrical conductivity (see sub-section 4.1.5.). The printing resolution of these inks are shown on Figure 4.14, comparing two different patterns, which were printed at RT using distinct cellulose binders with a concentration of pristine CFs of 10 % wt. For EC-based ink, the narrower printed line, with a width of 480 µm, was obtained for a screen pattern line width of 275 µm. For CMC-based ink, that value was 400 µm. The addition of the carbon solid content to binders' solution seems to decrease the printing quality of patterns in terms of minimal resolution.

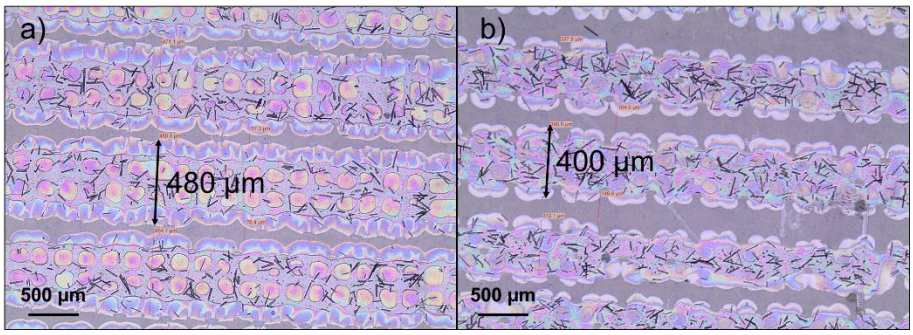

Figure 4.14 – Optical microscope images from the narrower and contiunous screen printed lines obtained from 5 % wt. EC (a) and 3 % wt. CMC (b) based inks with 10 % carbon fibers.

4.1.5. Electrical conductivity of printed patterns

Several samples were prepared in order to understand the influence of various parameters, such as the inks' composition, (including, carbon material and cellulose binder used and their respective concentration), number of printing passes, CF morphology and drying conditions performed between each printing pass, on their electrical performance.

4.1.5.1. Influence of number of prints on electrical conductivity

As depicted in Figure 4.15 and Figure 4.16, it is demonstrated a clear influence of the number of printing passes (from 1 to 10) and pristine CFs content (1 %, 5 % and 10 %) on the surface profile of the screen printed films based on CMC and EC, respectively. Each layer of the printed films was deposited using square patterns, and dried at RT conditions for 15 min. Furthermore, these results were correlated with the electrical resistivity of the screen printed films as function of the number of printed layers, as shown in Figure 4.16.

In general, it is visible a cellulose-based matrix hosting the CFs, being the CFs evenly distributed within the matrix of the printed films. For low concentration of CFs (< 5 % wt.), it is not observed a direct contact between the fibers, even after 10 printing passes, which will result on a highly resistive printed film. Although, it is visible a significant increase on CFs density with the number of printing passes, and the printed films became electrical conductive after 9 printing passes for a CFs content of 5 % wt. More interesting results were obtained for the printed films prepared from CMC and EC-based electroconductive inks with high levels of CFs (10 % wt.) after 4 and 5 printing passes, respectively. It is notorious the existence of a direct electrical contact between the conducting materials in the printed pattern, forming percolation paths.

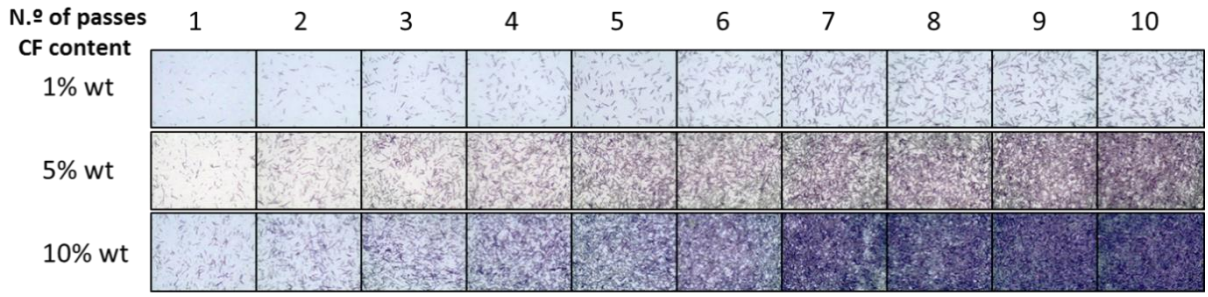

Figure 4.15 – Optical microscope images of the screen printed films after various printing passes (from 1 to 10), prepared from CMC based electroconductive inks with different concentrations of CFs (1 %, 5 % and 10 % wt.).

After 4 printing passes, the electroconductive printed film based on CMC exhibits an electrical resistivity around 10.06 Ωcm. On the other hand, a resistivity of 19.22 Ωcm was measured for a printed film based on EC, after 5 printing passes. It continues to decrease as the number of printing layers increases, stabilizing after 8 printing passes. After 10 printing passes, the resistivity of the films decreases to 1.03 and 1.81 Ωcm, for CMC and EC-based electroconductive inks, respectively, considering these results, the CFs proportion was fixed at 10 % wt.

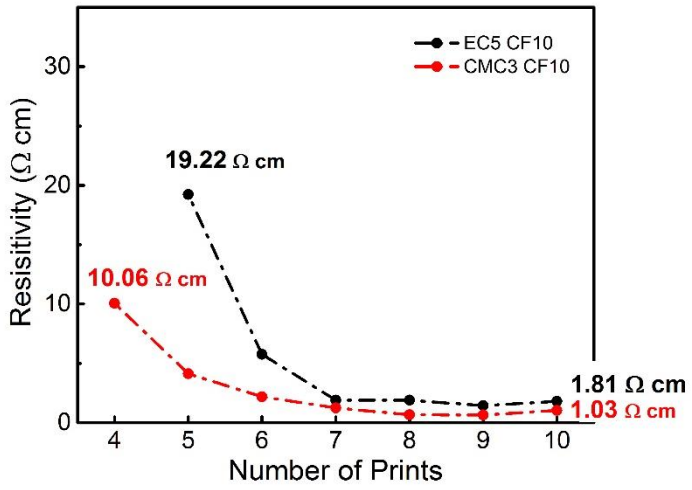

Figure 4.16 – Resisitivity of screen printed patterns of CMC and EC based inks with 10 % wt. as received carbon fibers with increasing number of printing passes.

The resistivity of screen printed films of MWCNTs was studied as a function of printed layers for CMC and EC as binder of the formulated ink. Since MWCNTs are much smaller than CFs, the printing was performed using a mesh model of 120. The formulation of this inks was based on the binder proportions already used before to produce conductive CFs inks (as 3 % wt. of CMC and 5 % wt. for EC), and the MWCNTs proportion was fixed at 0.5 % wt. The formulation of similar inks with different binder solutions was performed in order to compare both electrical performance and quality of printed patterns. If in one hand EC has been reported in literature as an excellent binder for screen printing applications, on the other hand no further studies were found about carbon nanostructures dispensability on EC's solution. The aggregation of NPs and formation of bundles can compromise electrical performance and, although its printability have never been studied in this context, CMC was already reported as an excellent dispersant of CNTs structures. For this reason, the performance of both cellulose derivatives was compared.

Figure 4.17 shows optical microscope image of the screen printed films surface with 1 to 10 layers. Comparing the different patterns, although the same proportion of MWCNTs have been used for both ink, EC based ink reveal patterns with slightly bright tones. This can be related to possible aggregation of MWCNT structures. The higher electrical resistivity (Figure 4.18) for EC based ink seems to corroborate this theory, since aggregation of electrical structures may reduce the percolation paths that allow electrical conduction on the film.

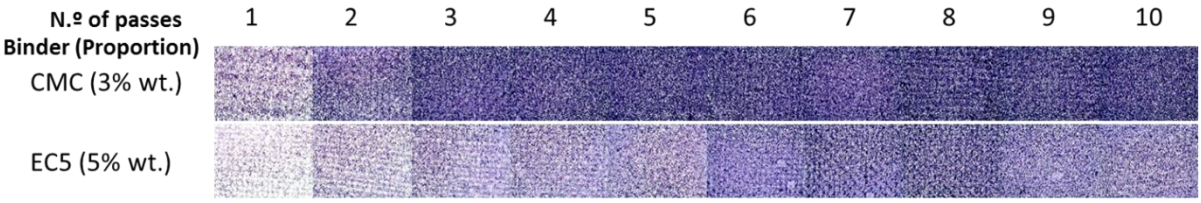

Figure 4.17 - Optical microscope images of the screen printed films after various printing passes (from 1 to 10), prepared from CMC and EC based electroconductive inks of 0.5 % wt. of MWCNTs.

MWCNTs based inks reveals a significantly better electrical performance than CF based inks, as long as one printing passe is suficient to form electrical conductive paths, achieving a resistivity of 22.44 and 0.57 Ωcm for only one printing layer for EC and CMC inks respectively, which is a better value than the one achieved for 10 printing layers with CF based ink. Its important to remember that not only MWCNTs conductivity is higher than CFs, but also the ratio between mesh oppening and carbon structures lengh is quite high and the clogging or prisioning of this structures on the mesh is not a problem, beeing those facts suficient justifications to explain the higher conductivity achived. As observed on previous study of CFs patterns, the electrical resisitivity of the screen printed patterns after several printing layers is caracterized by two different regions. In the first region, were resisistivity drops fast with increasing printing layers, electrical conduction is essenctially limited by the relatively low number of existing percolation pathhs, competing with the contact resistance and intrinsic defects of the carbon structures. In the second region, resisitivity stabilizes at a value characteristic of the conductive material type. The transition between these regions occurs for 3 or 4 printing passes, , with a resisitivity of EC and CMC is 10.67 and 0.26 Ωcm respectively. Since the same electroconductive material was used for both inks at the same proportion, here again the agregation of MWCNTs in EC solution is pointed as the cause for this higher resistivity value.

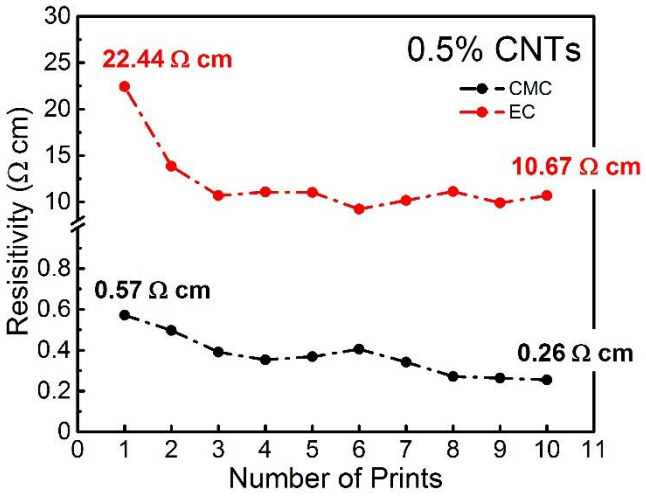

Figure 4.18 – Resisitivity of screen printed patterns of CMC and EC based inks with 0.5 % of MWCNTs with increasing number of printing passes.

4.1.5.2. Influence of carbon structures morphology on electrical conductivity

A study was carried out in order to understand the influence of CFs morphology adopted for formulation of the inks on electrical performance. As it was mentioned in sub-section 4.2.1., milling proved to be a successful mechanical treatment for reduction of the length size of the CFs, as an attempt to improve their printability. Thus, it is expected to increase the density of CFs in the printed film, creating a conductive path along and between the CFs with the final goal of enhancing the electrical performance of the printed film. However, the implementation of such treatments alters drastically CFs morphology, being some individual CFs severely damaged, which will not contribute for an efficient electrical conduction.

Figure 4.19 shows optical microscope images of the printed patterns, where no significant difference on CFs density can be observed. Figure 4.20 a-b show the electrical behavior of the printed films with various printing passes, considering the cellulose binder used, where pristine and milled CFs are compared for a fixed content of 10 % wt.

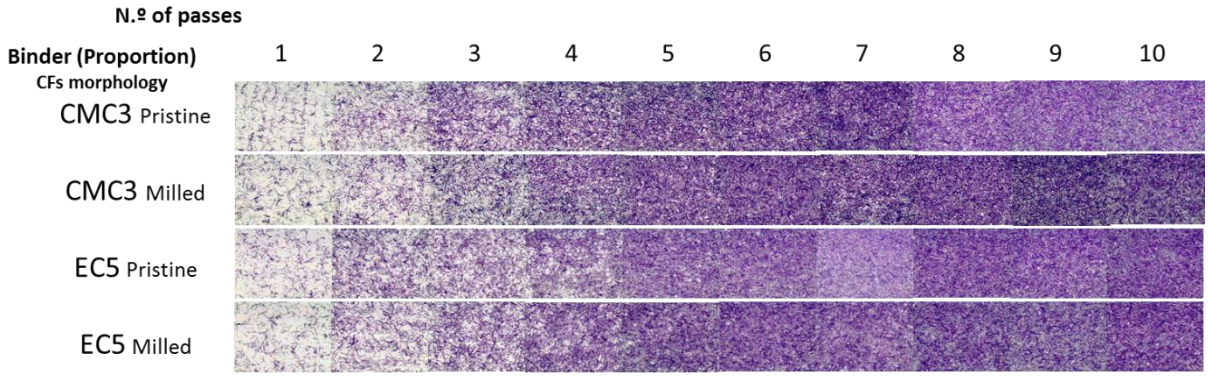

Figure 4.19 - Optical microscope images of the screen printed films after various printing passes (from 1 to 10), prepared from CMC and EC and pristine and milled CFs.

For the CMC ink with milled CFs, percolation paths seems to form after one additional printing step than for as received CFs. This probably happen because the shorter length of the fibers doesn't provides such a great range of contact points between neighboring fibers, requiring an extra layer for electrical conduction to occur. The resistivity seems to stabilize after 8 passes being 1.24 and 1.03 Ωcm for as received and milled CFs, respectively, after 10 printing passes.

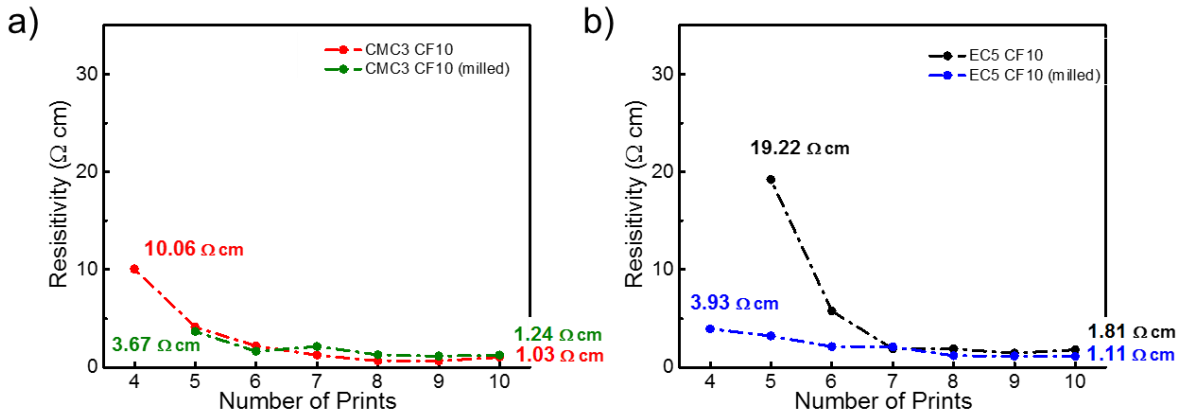

Figure 4.20 – Comparison of electrical performance of CMC and EC based inks prepared with as received and mechanically treated CFs.

The comparison of resistivity of EC based inks in on Figure 4.20b. In this case more passes are required to have percolation in printed films with as received fibers. This is associated to a worst dispersability of the fibers in the EC that resulting in some agglomeration. If big fibbers agglomerate it will be more difficult to pass through the mesh when comparing with agglomerates of small fibers. Again the resistivity seems to stabilize after 7-8 passes, presenting a value of 1.81 and 1.11 for as received and milled fibers, respectively, after 10 printing passes.

4.1.5.3. Influence of drying conditions on electrical conductivity

From previous TGA and FTIR analysis on sub-sections 3.1.1. and 3.1.4., two drying methods were applied to printed films from CMC based inks. The first method consists on drying at RT for 15 min and second method consist on drying at 120 ºC on an oven. The influence of the two drying methods in the electrical performance of films from one to 10 printing passes is shown on Figure 4.21. Here again is possible to see a different behavior for pristine and milled CF based inks. The as received pristine CF based inks have a great increase in electrical resistivity when dried at 120 ºC however, milled CF based ink electrical performance doesn't show any significant variation. Here again, one would expect an increase in conductivity by better evaporation of solvents (see Figure 4.13 sub-section 3.1.4.). Since TGA analysis of inks confirms the stability under this range of temperatures, further investigation should be carried out.

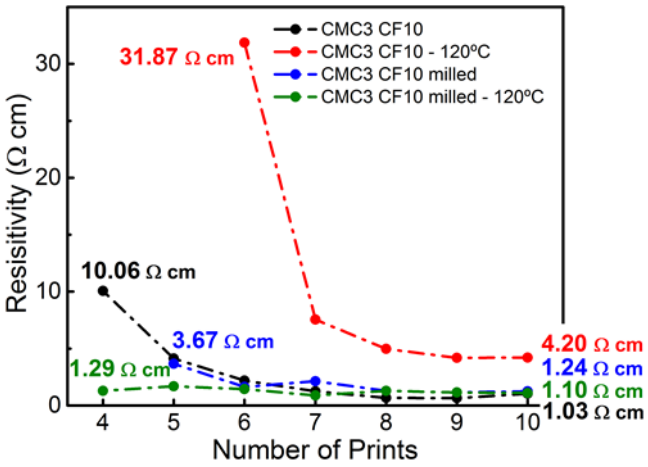

Figure 4.21–Influence of drying methods on electrical performance of the screen printed filmsfrom CMC based inks.

The results presented in this sub-section allowed to conclude that the combination of 3 % wt. of CMC in aqueous solution and 10 % wt. of pristine CFs is the formulation that results in a higher conductivity, after a sequence of 10 printing passes. For this reason, further studies were carried using only this ink, at which was given the name CMC3 CF10 (see Annex N a).

4.1.6. Reliability, flexibility, stress conditions and temperature influence on electrical conductivity of screen printed films

As stated before, the previous study of electrical properties of conductive films was performed inside a glove box, under controlled conditions of humidity and temperature. In an attempt to predict electrical resistivity under normal environmental conditions, electrical measurements of 8 samples of screen printed films with 10 layers of CMC3 CF10 ink were selected and its resistivity was measured with 4 point probe technique (48 % RH and 25.2 ºC). Figure 4.22 shows the resistivity values of each sample, with an average of 4.69 Ωcm, and a standard deviation of 0.95 Ωcm. The increase in the resistivity value is due to the increase of relative humidity of air, which contribute to adsorption of water molecules into the film structure that can swell causing expansion and reduction of contact point between fibers. Considering the average thickness of the films (37.43 µm, see Annex O) and using the expression 1 (Annex P) the sheet resistance value for ten layers of CMC3 CF10 films is estimated to be 1.253 kΩ/□.

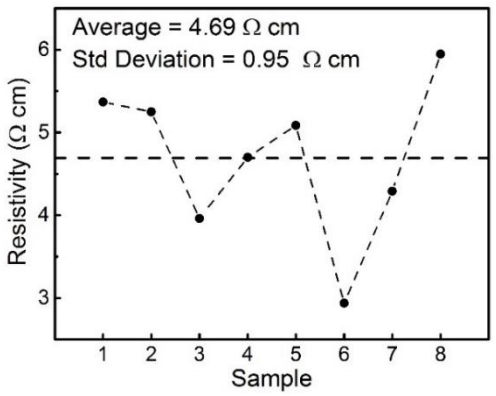

Figure 4.22 – Resisitivity of screen printed films from CMC3 CF10 ink dried at RT.

The electrical performance of materials intended for flexible electronics should be predicted under certain constraints. For that reason, printed films were subjected to a range of temperatures until 90 ºC to study electrical behavior under this conditions, as well as different bending radius and several bending cycles. The set-up used to measure electrical resistance dependence of temperature is shown on Figure 4.23 a) and automatic machine built to simulate stressing conditions with repeated bending cycles is shows on Figure 4.23b).

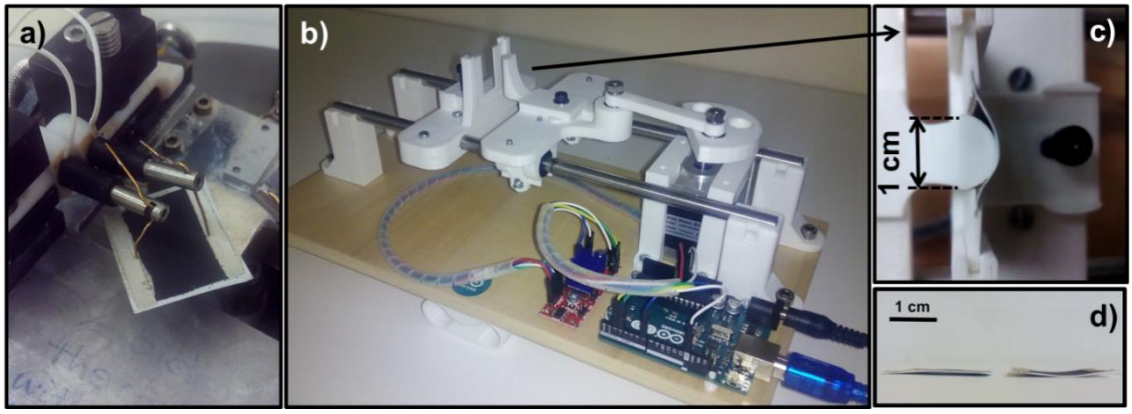

Figure 4.23–a) Assembly used to measure temperature inlfuence on electrical resistance of printed film; b) 3D printed automatic machine used to simulate stress conditions with repeated bending cycles; c) Detail of 0.5 cm radius stick; d) aspect of FS3 with printed film after 1000 cycles of bending on substrate side (left) and film side (right).

The influence of amplitude of bending on electrical performance was tested for tensile (means that the printing pattern is turned outside) and compressive (means that the printing pattern is turned inside) bending through several angles, using cylinders with different radius (1.85, 1.34 and 0.50 cm). Figure 4.24 shows the relative resistance of patterns during bending with specified radios. One can see the increase on resistance of about 2.41 times the initial value for tensile bending direction on extreme case of bending, which is due to the formation of cracks caused by the distention of the film. Oppositely, the decrease of resistance for 0.45 of the initial value for compressive bending is related to the compression of the film, which allows the formation of new conductive paths.

To further studies of electrical performance under stress conditions repeated bending over 1000 cycles with a fixed angle was performed, using a cylinder with a radius of 5 mm, from both sides of paper. Both tensile and compressive stress affect significantly the electrical performance. However, and contrary to what would be expected, resistance decreases after bending cycling. After 1000 cycles of compressive stress, resistance decreases for 65 % the initial value while for tensile bending, resistance decreases for 53 %. The decreasing of resistance is probably related to a rearrange and to the formation of more points of contact between fibers from different layers because of the twisting applied to the film.

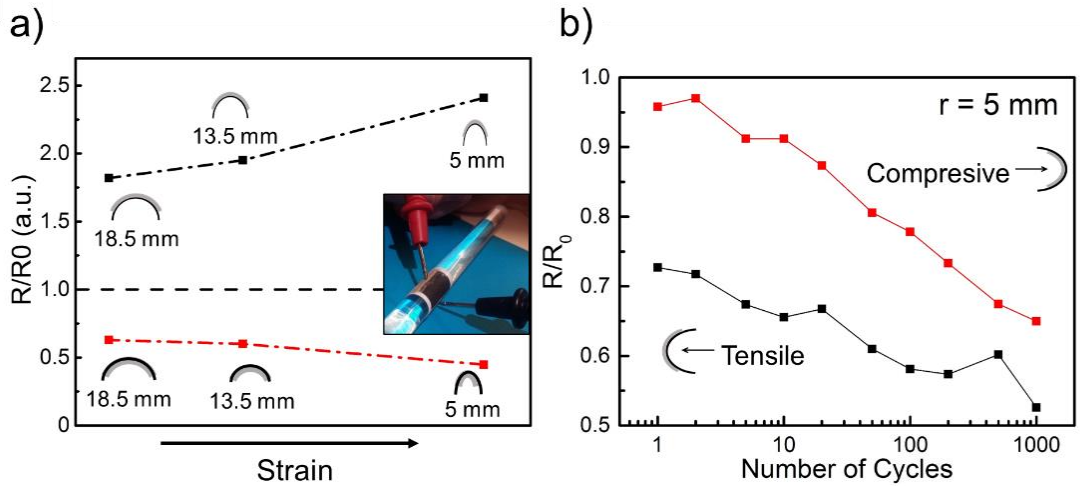

Figure 4.24 – a) Relative resistance of printed patterns in order to folding angle, here demonstrated using cylinder with several diameters (Measurement conditions: 38% air humidity and 25.6ºC); b) Relative resistance of patterns of 10 screen printed layers of ink CMC3 CF10 after repeated cycles of bending using an automatic machine (Figure 4.23 b) with 5 mm of radius of curvature. (Measurement conditions: 38% air humidity and 25.6ºC).

Electrical resistance of printed film of ink CMC3 CF10 was studied from RT (25.8 ºC) until 367 K (94 ºC) and it was observed that resistance decreased to half of its initial value (Figure 4.25), demonstrating a negative resistance coefficient. Such behavior is characteristic of non-metals and semiconductors and has also been reported on carbon fiber composites. [94] It is believed that electrical conduction in such composite is described by hopping theory, since structural defects on fibers and its interfaces and the resultant scattering effect decreases the relevance of tunneling between fibers. [95]

Temperature increases the number of carriers available for conduction and also contributes for the evaporation of adsorbed water on the cellulosic matrix (cellulose compounds can trap a considerable amount of water in its structure, about 15 % wt. according to TGA analysis of CMC membrane in Annex Q), allowing to increase the conductivity of the material. According to the data from TGA analysis, CMC is stable under the range of temperature applied however, the thermal expansion of CMC increase the distance between neighboring fibers and this is visible as a clear change in the conduction behavior and from the decreasing in the slope of the plot. The activation energy (E_a) calculated from the linear regression of data (Annex R) and from expression 2 on Annex S of the two different regions on graphic reveals a higher activation energy value for low temperatures (0.12 eV) and a lower value for high temperatures (0.08 eV), and defines the transition from the regime were expansion of the matrix influences the conduction in the printed layers.

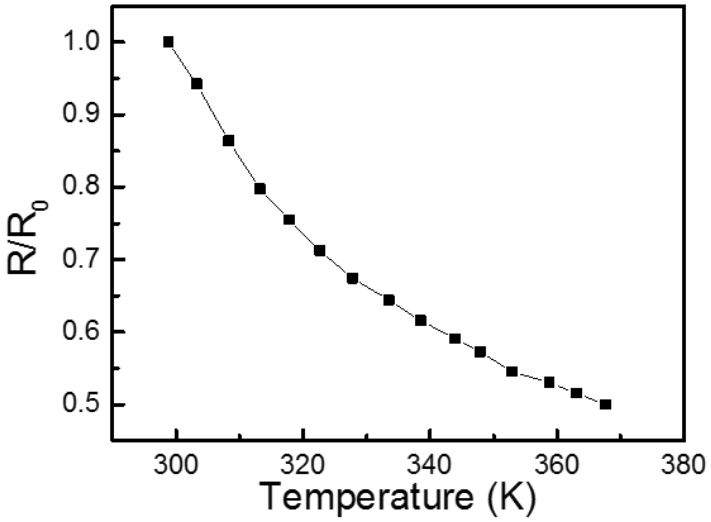

Figure 4.25–Evolution of electrical resistance of patterns with10 screen printed layers of ink CMC3 CF10.

4.1.7. Application to electric circuits

As proof of concept, the developed conductive inks (namely the CF based) was implemented on a simple circuit to light a LED. Figure 4.26 a) shows the developed screen printed circuit using a commercial silver paste as conductive tracks and the developed CF and aqueous based ink as resistive element (CMC3 CF10). The folding of the paper act as a switch, turning the LED ON and OFF (Figure 4.26 b). The device was switched with 3 V, which allows the use of a battery.

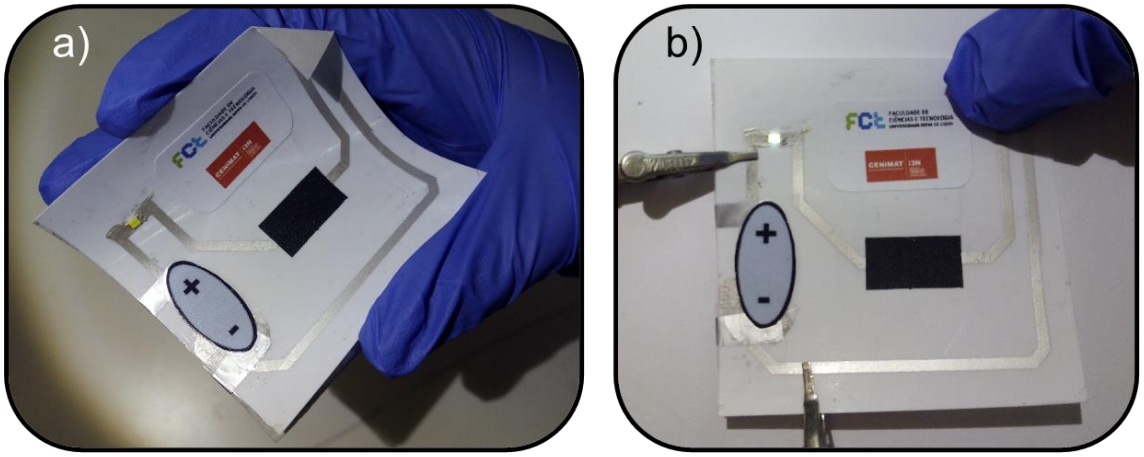

Figure 4.26 –Electric circuit to light a LED fabricated by screen printing using a commercial silver ink as connectors and the devolped CF aqueous based ink (CMC3 CF10) on the paper FS3 (a). Folding the paper turns the LED ON (b).

4.2. Cellulose-based hydrogels applied as the gate dielectric in electrolyte-gated transistors for printed electronics

This chapter is dedicated to the electrochemical characterization of the developed hydrogel electrolytes and to its implementation in EGTs. Electrolytes were prepared as described on chapter 3.2., through the dissolution of 4 and 8 % wt. of MCC in the new low temperature solvent system containing LiOH and Urea (MCC4 and MCC8). To the best of our knowledge, the dissolution of this type of cellulose using this solvent system was never reported on literature, neither has been applied as electrolyte in EGT devices. So, the main objective was not to make an exhaustive study on the subject, but to demonstrate that is possible to do both, by the implementation of the electrolyte in an EGT device as proof of concept, which has been successfully accomplished.

4.2.1. Electrochemical impedance spectroscopy characterization of the cellulose based electrolytes

The electrochemical impedance spectroscopy (EIS) is a precious measuring tool used to determine some important electrical properties of ionic materials. [66] The material is sandwiched between two metal electrodes on a parallel plate configuration (see Figure 4.27 a) called electrochemical cell (EC) and the measuring procedure consists on applying an AC voltage with a range of different frequencies (f) to the electrochemical cell and measure the total impedance of the system (Z). The application of a potential in the electrodes promotes migration of oppositely charged ions to the electrolyte interfaces, forming the EDL. The charge distribution on EDL is described by CGS model (Goüy-Chapmen-Stern) and divides the EDL in two different layers (see Annex T, with the one closer to the electrode (called Helmholtz layer) being only a few angstroms thick and responsible for a very steep loss of potential and the other layer extending relatively far in the electrolyte, with the total capacitance of the double layer being generally in the order of the tens of μFcm^{-2}. [96] From this data obtained from EIS measurements is possible to obtain precious information about ion migration, EDL formation, dielectric capacitance (C_i) and charge carrier mobility. To describe the behavior of this EC, a circuit model with reasonable fitting of the acquired data was studied in detail.

4.2.2. Equivalent circuit model

In order to properly describe the electrochemical behavior of the electrolyte, is necessary to find an equivalent electrical circuit model. This model is helpful in determining parameters such as bulk resistivity (ρ), ionic conductivity (σ_i), bulk capacitance (C_b) and EDL capacitance (C_{DL}). From several circuit models, the simplified Randel cell is the most commonly used model and the starting point to more complex ones. This circuit is composed of a resistance (R_{ext}) in series with a parallel RC circuit (represented on Figure 4.27 b). The R_{ext} is associated with the contact resistance from the electrodes while the RC circuit represents the electrolyte and its composed of a resistance R_b representing the bulk resistance and a non-ideal capacitive component, the so called constant phase element (CPE), standing for the C_{DL}. According to several authors, the non-ideal capacitive behavior of C_{DL} is associated to interface roughness and inhomogeneities however, its physical basis to date is only poorly understood.[97] The CPE include both capacitive behaviors at higher and lower frequencies, caused by dipole relaxation and the EDL formation, respectively.

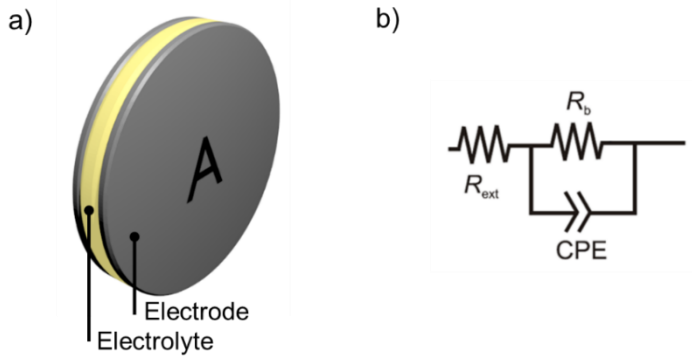

Figure 4.27–A scheme of the parallel plates configuration of electrochemial cell used for EIS measurements (a) and the equivalen circuit model used for fitting of aquired data (b).

The impedance magnitude and the phase angle were measured in the frequency range of 10^5 to 10^{-1} Hz. From Figure 4.28 is possible to see similar behaviors for both electrolytes MCC4 and MCC8 (with 4 and 8 % wt. of MCC, respectively). For higher frequencies, the phase shift between current and voltage is near 0º. The nonexistence of a phase delay is a characteristic behavior of a purely resistive element and is associated to ionic relaxation on electrolyte. As frequency decreases, a negative phase shift occurs and it reaches values near -90 º, suggesting progressive predominance of the capacitive behavior, for low frequencies. The transition between this two regions occurs at -45 º for a frequency near $3x10^2$ Hz and is associated to the EDL formation (for lower frequencies). Also, the decrease in capacitance associated to the destruction of the EDL and the frequency at which occurs limits the application on devices determining the fastest response time achievable in electrolyte gated transistors.

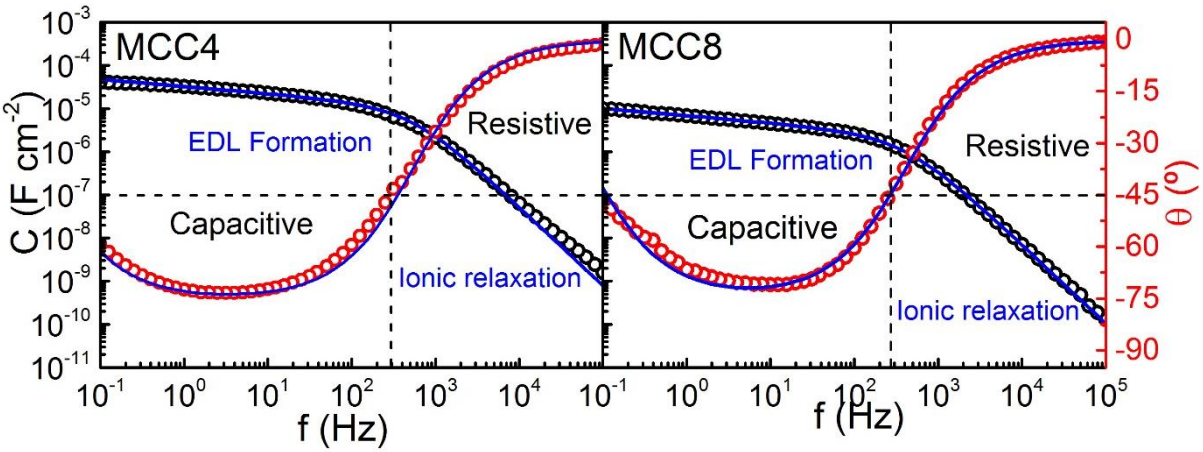

Figure 4.28 – Data obtained by EIS measurements (red and black circles) and respective fitting with Randel model (blue line) of MCC4 and MCC8 electrolytes.

As demonstrated on Figure 4.28, the fitting with Randel model describes properly the acquired data along all the frequency range whereby, there is no need for a further complex circuit. The characteristic parameters calculated from the fitting model are summarized on Annex U. From the obtained parameters and using expression 3 in Annex V, it's possible to obtain C_{DL} values of 12.10 and 2.62 μFcm^{-2} for MCC4 and MCC8 respectively. The lower capacitance value obtained for MCC8 is related to the higher mass content of MCC that prevents that a higher accumulation of charges takes place at Helmholtz region. However both calculated values (≥ 1 μFcm^{-2}) are characteristic of electrolytes. [73] Ionic mobility's of $3.56x10^{-7}$ and $5.57x10^{-7}$ Scm^{-1} obtained for MCC4 and MCC8 respectively (and calculated from expression 4 in Annex W) are very similar and such low values are intrinsically related with the low frequency at which transition from resistive to capacitive behavior occurs. With this model, α values of about 0.84 and 0.83 were obtained for MCC4 and MCC8 respectively, which gives both only an over 80% capacitive behavior. The incomplete semi-circle in Nyquist plots (Figure 4.29) shows a charge transfer occurring for lower frequencies than 10^{-1} Hz and reveals a high electrolyte bulk resistance, determined as $1.19x10^5$ and $1.96\ x10^5$ Ω by the fitting model for MCC4 and MCC8 respectively. The first charge transfer is related to interfacial resistance of electrodes and is found to be $2.47x10^1$ and $1.49x10^2$ Ω respectively.

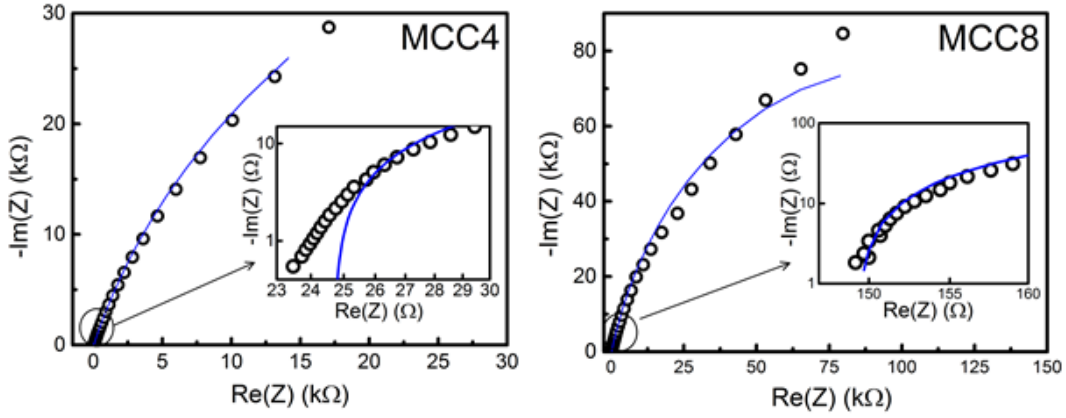

Figure 4.29 – Nyquist plot for MCC4 (a) and MCC8 (b) electrolytes.

The electrochemical stability of the electrolytes was evaluated between -2 and 2 V at a rate of 25 mV/s (Figure 4.30). MCC4 reveals some peaks near -0.8 and 0.9 V which can be related to water or urea dissociation. Meanwhile, the symmetry of these two peaks is an indication of a reversible reaction that in principle will not affect significantly the stability of operation of the electrolyte. The cyclic voltammogram also reveals a larger area for MCC4 electrolyte. This phenomenon can be related to a less packaged cellulosic matrix of MCC4, leading to a higher capacity of accommodate and retain ions on its structure.

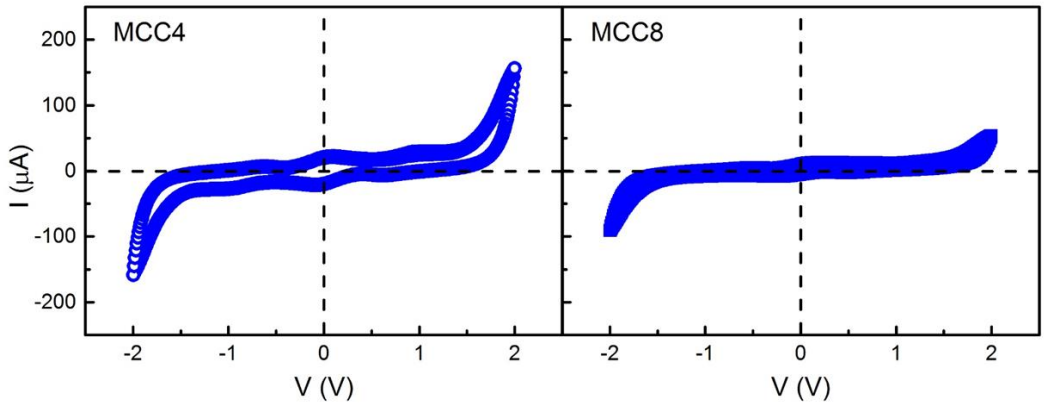

Figure 4.30 – Cyclic voltammogram of both MCC4 and MCC8 electrolytes on the cell performed at rates of 25 mV/s between -2 and 2 V.

4.2.3. Application to EGTs

An image of MCC4 and MCC8 electrolytes is shown in Annex N (b and c). These cellulose based electrolytes were implemented on a GIZO EGT with a planar configuration. The characterization was performed by applying a gate voltage (V_G) between -2 and 2 V to, with a constant drain to source voltage (V_{DS}) and measuring the drain to source current (I_D). The data obtained for EGTs using MCC4 and MCC8 as electrolytes is shown on Figure 4.31 and the calculated parameters are presented on Table 4.3 As stated before, the high capacitance of electrolytes is responsible for a high carrier concentration at semiconductor interfaces and allows a low operation voltage. A potential of 1.2 V and 1.4 V were found to be the lowest drain voltage (V_D) to operate MCC4 and MCC8 devices, respectively. The V_{ON} for both devices is a positive value, evidencing that this device behave as a normally off n-type transistor. The drain current in the off state of MCC4 device is lower than MCC8, which was expected since leakage current in MCC8 is about one order of magnitude higher and also due to the slight difference in the V_{DS} used in order to obtain positive values for I_D. Through the application of a positive gate voltage, the drain current of the device increases exponentially, showing a ON/OFF drain current ratio of 3.47×10^5 for MCC4 and 2.45×10^3 for MCC8. The higher ON current of MCC4 device against MCC8 can be related to the lower capacitance of MCC8 electrolyte, about one order of magnitude lower. A lower capacitance induces a lower carrier concentration in the semiconducting channel and is responsible for the lower ON current. The leakage current (I_G) in the ON state of both devices is in the same order of magnitude. This parameter is directly connected by the electric resistivity of the electrolyte that was also found to be similar.

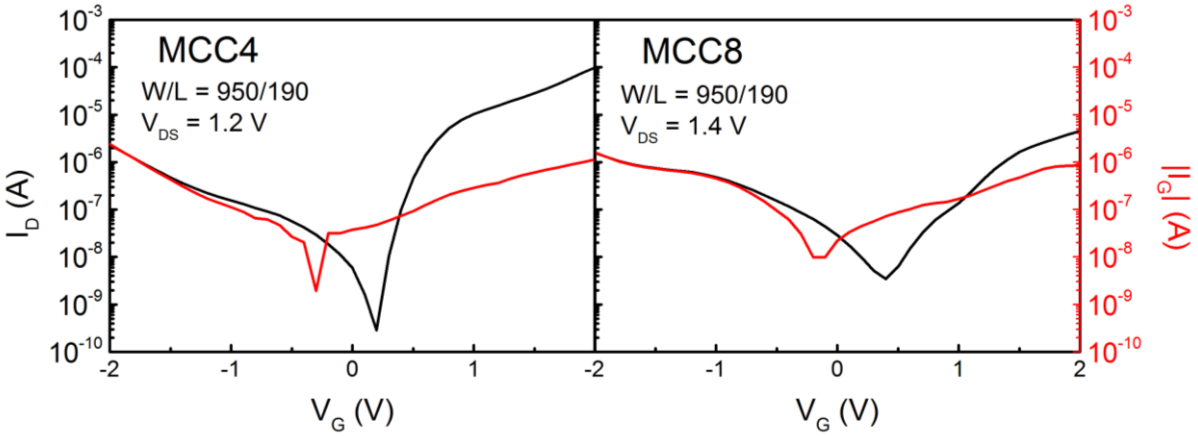

Figure 4.31 – Output curves from EGTs using MCC4 and MCC8 prepared solutions as electrolyte.

The mobility of charge carriers was calculated with expression 5 in Annex X, using the CDL determined above and is an order of magnitude larger for MCC4 device, reaching 2.94 $cm^2V^{-1}s^{-1}$ while it is 0.43 $cm^2V^{-1}s^{-1}$ for the device with MCC8. This difference is related to the capacitance of the electrolyte where C_{DL} in MCC4 is about 10 times higher than for MCC8, resulting in a higher charge accumulation of carriers in the semiconductor in the same V_{GS} range.

The subthreshold slope (SS) was calculated with expression 6 in Annex Y and indicates how fast is the transition between the ON and the OFF state of the device. The EGT with MCC4 presents a lower SS also as result of the higher C_{DL} when comparing with MCC8. Transconductance value was calculated from expression 7 on Annex Z.

Table 4.3 – Comparison of parameters between EGTs using MCC4 and MCC8 as electrolyte.

	W/L (µm/µm)	V_{DS} (V)	V_{ON} (V)	$I_{ON/OFF}$	SS ($Vdec^{-1}$)	gm (S)	μ_{LIN} ($cm^2V^{-1}s^{-1}$)
MCC4	950/190	1.2	0.2	$3.47x10^5$	$7.89x10^{-2}$	$2.15x10^{-4}$	2.94
MCC8	950/190	1.4	0.4	$2.45x10^3$	$2.93x10^{-1}$	$7.88x10^{-6}$	0.43

The thickness independence of the electrolyte capacitance is particularly interesting, aiming for the production of this devices by printing methods like screen printing (1-100 µm), without misleading the low voltage operation. Whereby, the successful implementation of the developed electrolytes opens doors for further investigation on its application in a fully printed cellulose based device.

5. CONCLUSIONS AND FUTURE PERSPECTIVES

In this work, two cellulose based composites for electro and ionic conduction were produced: eleconductive inks relying on carbon structures and cellulose derivatives were optimized for screen printing on cellulose-based substrates and lithium and microcrystalline cellulose based hydrogel electrolyte was applied on electrolyte gated transistor (EGTs). The development of electroconductive inks comprised the preliminary study of carbon structures (carbon fibers – CFs, and multi-walled carbon nanotubes – MWCNTs), the morphology of substrates and its affinity with inks solvent. The inks formulation was then followed by the optimization and electrical characterization of screen printed patterns. The electrochemical properties of the produced hydrogel electrolytes was studied and optimized for enhanced ionic conductivity and application on EGTs devices. The next topics are meant to discuss the final conclusions of this work and future perspectives.

5.1. Final conclusions

In this work, two cellulose based composites for electro and ionic conduction functionalities were developed. In the first topic, a low cost, water based and biodegradable CF based conductive ink was developed for application on resistive elements for printed electronics, in particular for application for screen printing technique. Enhancement of conductive properties was also achieved by using low loadings of MWCNTs.

Electroconductive inks based on cellulose derivatives carboxymethyl cellulose (CMC) and ethyl cellulose (EC) as binding agent and using carbon fibers (CFs) and multi-walled carbon nanotubes (MWCNTs) as conductive agents were successfully developed. Formulation of inks consists on either 3 % wt. of CMC or 5 % wt. of EC diluted on respective solvent system (ultrapure water and toluene:ethanol (80:20) respectively) and 10 % wt. of CFs or 0.5 % wt. of MWCNTs. This proportion of binding agents was found to be the best combination from several tested, for producing the narrowest uniform and continuous lines. Rheological measurements revealed shear thinning behavior for all inks, and viscosity values were also found to be in the range of suitable values for screen printing reported in literature [35][84], ranging from 14.78 – 71.23 and 4.32 – 7.48 Pas for EC and CMC, respectively, for a shear rate of 10^{-1} s^{-1}. The addition of conductive elements increases the viscosity values.

Carbons fibers (CFs) with a diameter of 7 µm and about 150 µm length were provided by FISIPE and used as electroconductive element on inks. The milling of CFs has proved to reduce significantly their length but also to damage its structure so, although it allows a higher density of fibers to pass through the mesh, it does not improve significantly the conductivity of patterns. The resistivity measurement of a single fiber revealed to be 1.30×10^{-3} Ωcm, and the contact resistance between two neighboring fibers of 0.91 kΩ. On the other hand, MWCNTs with about 1 to 4.3 µm and a diameter of 15 nm were also used as electroconductive element on inks and mixed with the binders CMC (3 % wt.) and EC (5 % wt.) in the proportion of 0.5 % wt. In such proportions, CMC reveled itself as a great dispersant agent for MWCNTs and, unlike EC, prevented the creation of large material aggregates and bundles.

Screen printing of formulated inks was performed on a cellulose-based substrate, which was selected for its relatively high superficial smoothness and good barrier properties derived from a nonporous polymeric coating, compatibility with used solvents and a good adhesion of the inks, and its thermal stability under the required range of temperatures.

For CF based inks, the best results were achieved for aqueous dispersion with 10 % wt. of pristine CFs and 3 % wt. of CMC dried at RT, revealing a resistivity of 1.03 Ωcm after 10 printing passes (measured at standard conditions: T = 25.2 ºC and RH = 48 %) and a resolution of patterns of 400 µm. CMC is highly hygroscopic so printed patterns revealed an average resistivity of 4.69 Ω cm at RT conditions (48 % RH and 25.2 ºC), corresponding to a to a sheet resistance of 1.253 kΩ/□. Folding tests performed at different bending radius revealed a decrease of resistivity while compressive strain is applied (about 45 % for a bending radius of 5 mm) and an increase of resistivity while tensile bending being applied (about 241 % for the same bending radius). After 1000 bending cycles, compressive and tensile strain were found to reduce resistivity of patterns to 65 % and 53 % of its initial value, respectively. Is was also found that resistivity of patterns decrease with temperature, dropping to about 50 % of its initial value for 94 ºC. MWCNTs based inks revealed a better electrical performance than CF based

inks, and best results were achieved while using 3 % wt. of CMC as binding agent and 0.5 % wt. of MWCNTs. Screen printed patterns presented a resistivity of 0.57 Ωcm after only one printing passage, and 0.26 Ωcm after 10 printing passes, measured at controlled RT.

In the second part of this work, cellulose base composites for enhanced ionic conduction was prepared, studied and applied as electrolyte layer in EGT devices. The synthetized cellulose based hydrogel electrolytes were prepared by dissolution of different proportions (4 and 8 % wt.) of microcrystalline cellulose (MCC) on an ionic solvent system composed of a mixture of lithium hydroxide and urea (4.6:15). EIS measurements revealed a double layer capacitance of 12.10 μFcm^{-2} which are in accordance with the values encountered in literature (≥ 1 μFcm^{-2}). [73] Ionic mobility of MCC4 electrolyte was found to be $3.56x10^{-7}$ Scm^{-1} and the destruction of electrical double layer occurred for frequencies higher than 284 Hz. Electrolytes were found to be stable under the range of potential applied (-2 to 2 V).

Electrolytes were successful implemented in EGT devices with a W/L of 5 and best results were achieved for MCC4, presenting a channel modulation for a minimum V_D of 1.2 V, showing a V_{ON} of 0.2 V, a ON/OFF current ratio ($I_{ON/OFF}$) of $3.47x10^5$, with OFF state presenting currents on the order of 10^{-10} A and leakage currents (I_G) in the order of µA in the ON state. The linear mobility and the subthreshold slope were found to be $2.75x10^{-4}$ $cm^2V^{-1}s^{-1}$ and $7.89x10^{-2}$ $Vdec^{-1}$, respectively.

5.2. Future perspectives

This work showed great improvements in the area of printed electronics and advanced functional cellulose composites. Combining the both developed composites in the fabrication of an entirely printed and cellulose based EGT device and even a fully printed and cellulose based electronic circuit is a reality that will be possible to achieve in a near future. For that, a lot of work can be done and it's described on the line below.

Produced patterns from the developed inks along work not always showed a great reproducibility. Screen printing is known by its simplicity, reproducibility and reliability however, the different parameters introduced by the operator during the printing steps, like the force and velocity applied and the angle of squeegee can greatly influence the quality of patterns and as a consequence, the electrical performance. The more obvious way to have control on such parameters is by using an automatic screen printing machine which allows not only to fix them but also to have optimized values for each ink. Also another factor that was proven to influence the electrical performance of inks was the relative air humidity and room temperature. Cellulose chain is hygroscopic by nature and to minimize the effects of fluctuating ambient conditions, a proper encapsulation should be developed as a barrier to maintain as constant as possible. Another possible approach may be the use of another biopolymer chitosan, as it was proven to reduce the changes in the water content.

Further studies for enhanced conductivity of inks should be carried out by increasing the load content of conductive agents, whether CFs or MWCNTs. Also, the dispersive and stabilizer properties demonstrated by CMC and EC for the carbon structures and its interesting rheological properties opens space for future investigation on the use of alternative conducting or semiconducting agents for screen printing. For the same reasons, this compounds have potential for use on other applications, in particular other printing techniques, by varying the amount of binder content.

The chemical stability of carbon's nature also allows the implementation of developed electroconductive inks as electrode on chemically unstable devices, in particular EGTs, where addressing of the electrolyte is often difficult to handle when using metals.

The dissolution method employed to synthetize the hydrogel electrolyte produced good results and the same approach can be used in the future do dissolve other types of cellulose from different sources and to produce electrolytes for study in application on EGTs, electrochoromic displays or smart windows. A similar dissolution method developed by the same researches can also be studied and applied to this applications however, the use of Na^+ instead on Li^+ doesn't seem to have much advantages since the large size of Na^+ atoms reduces its mobility.

The stability of operation of the EGT device when subjected to different conditions of temperature and humidity should also be subject of study and a proper encapsulation should be developed to avoid complete dehydration of the composite (extreme drying of hydrogels gives place to a powdery solid residue).

6. BIBLIOGRAPHY

[1] J. Liu, C. Yang, H. Wu, Z. Lin, Z. Zhang, R. Wang, B. Li, F. Kang, L. Shi, and C. P. Wong, "Future paper based printed circuit boards for green electronics: fabrication and life cycle assessment," *Energy Environ. Sci.*, vol. 7, no. 11, pp. 3674–3682, Aug. 2014.

[2] D. Tobjörk and R. Österbacka, "Paper electronics," *Adv. Mater.*, vol. 23, no. 17, pp. 1935–1961, 2011.

[3] L. Pereira, D. Gaspar, D. Guerin, a Delattre, E. Fortunato, and R. Martins, "The influence of fibril composition and dimension on the performance of paper gated oxide transistors.," *Nanotechnology*, vol. 25, no. 9, p. 094007, 2014.

[4] S. Thiemann, S. J. Sachnov, F. Pettersson, R. Bollström, R. Österbacka, P. Wasserscheid, and J. Zaumseil, "Cellulose-based ionogels for paper electronics," *Adv. Funct. Mater.*, vol. 24, no. 5, pp. 625–634, 2014.

[5] J. Shokri and K. Adibki, "Application of Cellulose and Cellulose Derivatives in Pharmaceutical Industries," in *Cellulose - Medical, Pharmaceutical and Electronic Applications*, InTech, 2013, pp. 47–66.

[6] B. Lindman, G. Karlström, and L. Stigsson, "On the mechanism of dissolution of cellulose," *J. Mol. Liq.*, vol. 156, no. 1, pp. 76–81, Sep. 2010.

[7] J. Cai, L. Zhang, S. Liu, Y. Liu, X. Xu, X. Chen, B. Chu, X. Guo, J. Xu, H. Cheng, C. C. Han, and S. Kuga, "Dynamic Self-Assembly Induced Rapid Dissolution of Cellulose at Low Temperatures," *Macromolecules*, vol. 41, no. 23, pp. 9345–9351, Dec. 2008.

[8] X. Luo and L. Zhang, "New solvents and functional materials prepared from cellulose solutions in alkali/urea aqueous system," *Food Res. Int.*, vol. 52, no. 1, pp. 387–400, Jun. 2013.

[9] Q. Yang, H. Fukuzumi, T. Saito, A. Isogai, and L. Zhang, "Transparent Cellulose Films with High Gas Barrier Properties Fabricated from Aqueous Alkali/Urea Solutions," *Biomacromolecules*, vol. 12, no. 7, pp. 2766–2771, Jul. 2011.

[10] S. Zhang, F.-X. Li, J. Yu, and Y.-L. Hsieh, "Dissolution behaviour and solubility of cellulose in NaOH complex solution," *Carbohydr. Polym.*, vol. 81, no. 3, pp. 668–674, Jul. 2010.

[11] H. Águas, T. Mateus, A. Vicente, D. Gaspar, M. J. Mendes, W. a. Schmidt, L. Pereira, E. Fortunato, and R. Martins, "Thin Film Silicon Photovoltaic Cells on Paper for Flexible Indoor Applications," *Adv. Funct. Mater.*, p. n/a–n/a, 2015.

[12] A. Vicente, H. Águas, T. Mateus, A. Araújo, A. Lyubchyk, S. Siitonen, E. Fortunato, and R. Martins, "Solar cells for self-sustainable intelligent packaging," *J. Mater. Chem. A*, vol. 3, no. 25, 2015.

[13] A. C. Baptista, J. I. Martins, E. Fortunato, R. Martins, J. P. Borges, and I. Ferreira, "Thin and flexible bio-batteries made of electrospun cellulose-based membranes," *Biosens. Bioelectron.*, vol. 26, no. 5, pp. 2742–2745, Jan. 2011.

[14] A. C. Marques, "Desenvolvimento de um sensor colorimétrico em papel para a deteção de bactérias eletroquimicamente ativas," Master Thesis, Departamento de Ciências dos Materiais, FCT UNL, Portugal (2014).

[15] R. Martins, P. Barquinha, L. Pereira, N. Correia, G. Gonçalves, I. Ferreira, and E. Fortunato, "Write-erase and read paper memory transistor," pp. 2008–2010, 2008.

[16] E. Fortunato, N. Correia, P. Barquinha, L. Pereira, G. Goncalves, and R. Martins, "High-performance flexible hybrid field-effect transistors based on cellulose fiber paper," *IEEE Electron Device Lett.*, vol. 29, no. 9, pp. 988–990, 2008.

[17] D. Gaspar, S. N. Fernandes, a G. de Oliveira, J. G. Fernandes, P. Grey, R. V Pontes, L. Pereira, R. Martins, M. H. Godinho, and E. Fortunato, "Nanocrystalline cellulose applied simultaneously as the gate dielectric and the substrate in flexible field effect transistors," *Nanotechnology*, vol. 25, no. 9, p. 094008, Mar. 2014.

[18] G. Rodrigues, "Towards printed carbon nanotube transistors on paper substrates," Master Thesis, Departamento de Ciências dos Materiais, FCT UNL, Portugal (2014).

[19] M. Ângelo and P. Soares, “Control System for Actuation and Sensing in Digital Microfluidics Devices,” Master Thesis, Departamento de Ciências dos Materiais, FCT UNL, Portugal (2014).

[20] D. C. De Matos, “Digital Microfluidics on Paper,” Master Thesis, Departamento de Ciências dos Materiais, FCT UNL, Portugal (2014).

[21] V. Alexandre and V. Rodrigues, “Digital Microfluidic devices : the role of the dielectric layer,” Master Thesis, Departamento de Ciências dos Materiais, FCT UNL, Portugal (2014).

[22] Z. Shi, G. O. Phillips, and G. Yang, “Nanocellulose electroconductive composites,” *Nanoscale*, vol. 5, no. 8, p. 3194, 2013.

[23] Y. Y. Huang and E. M. Terentjev, “Dispersion of Carbon Nanotubes: Mixing, Sonication, Stabilization, and Composite Properties,” *Polymers (Basel).*, vol. 4, no. 4, pp. 275–295, Jan. 2012.

[24] A. Kamyshny and S. Magdassi, “Conductive Nanomaterials for Printed Electronics,” *Small*, vol. 10, no. 17, pp. 3515–3535, Sep. 2014.

[25] Y. Gao, W. Shi, W. Wang, Y. Leng, and Y. Zhao, “Inkjet Printing Patterns of Highly Conductive Pristine Graphene on Flexible Substrates,” *Ind. Eng. Chem. Res.*, vol. 53, no. 43, pp. 16777–16784, Oct. 2014.

[26] N. Minami, Y. Kim, K. Miyashita, S. Kazaoui, and B. Nalini, “Cellulose derivatives as excellent dispersants for single-wall carbon nanotubes as demonstrated by absorption and photoluminescence spectroscopy,” *Appl. Phys. Lett.*, vol. 88, no. 9, p. 093123, 2006.

[27] L. Jabbour, D. Chaussy, B. Eyraud, and D. Beneventi, “Highly conductive graphite/carbon fiber/cellulose composite papers,” *Compos. Sci. Technol.*, vol. 72, no. 5, pp. 616–623, Mar. 2012.

[28] G. TIBBETTS, M. LAKE, K. STRONG, and B. RICE, “A review of the fabrication and properties of vapor-grown carbon nanofiber/polymer composites,” *Compos. Sci. Technol.*, vol. 67, no. 7–8, pp. 1709–1718, Jun. 2007.

[29] A. Das, T. M. Schutzius, I. S. Bayer, and C. M. Megaridis, “Superoleophobic and conductive carbon nanofiber / fluoropolymer composite films,” *Carbon N. Y.*, vol. 50, no. 3, pp. 1346–1354, 2011.

[30] K. Suganuma, *Introduction to Printed Electronics*, vol. 74. New York, NY: Springer New York, 2014.

[31] J. Perelaer, P. J. Smith, D. Mager, D. Soltman, S. K. Volkman, V. Subramanian, J. G. Korvink, and U. S. Schubert, “Printed electronics: the challenges involved in printing devices, interconnects, and contacts based on inorganic materials,” *J. Mater. Chem.*, vol. 20, no. 39, p. 8446, 2010.

[32] T. C. Li, R. C. Chang, and Y. C. Li, “Ink jet printed thin films on glass and polyimide substrates,” *Trans. Can. Soc. Mech. Eng.*, vol. 37, no. 3, pp. 873–883, 2013.

[33] D. Buzby and A. Dobie, “Fine Line Screen Printing of Thick Film Pastes on Silicon Solar Cells,” *Int. Microelectron. Assem. nd Packag. Soc.*, no. 610, 2008.

[34] J. Chang, X. Zhang, T. Ge, and J. Zhou, “Fully printed electronics on flexible substrates: High gain amplifiers and DAC,” *Org. Electron.*, vol. 15, no. 3, pp. 701–710, Mar. 2014.

[35] P. J. Wojcik, “Printable organic and inorganic materials for flexible electrochemical devices.” Doctoral Thesis, Departamento de Ciências dos Materiais, FCT UNL, Portugal (2013).

[36] H. J. van de Wiel, Y. Galagan, T. J. van Lammeren, J. F. J. de Riet, J. Gilot, M. G. M. Nagelkerke, R. H. C. a T. Lelieveld, S. Shanmugam, A. Pagudala, D. Hui, and W. a Groen, “Roll-to-roll embedded conductive structures integrated into organic photovoltaic devices,” *Nanotechnology*, vol. 24, no. 48, p. 484014, Dec. 2013.

[37] R. Xiong, Y. Han, Y. Wang, W. Zhang, X. Zhang, and C. Lu, “Flexible, highly transparent and iridescent all-cellulose hybrid nanopaper with enhanced mechanical strength and writable surface,” *Carbohydr. Polym.*, vol. 113, pp. 264–271, 2014.

[38] L. Hu, G. Zheng, J. Yao, N. Liu, B. Weil, M. Eskilsson, E. Karabulut, Z. Ruan, S. Fan, J. T. Bloking, M. D. McGehee, L. Wågberg, and Y. Cui, “Transparent and conductive paper from nanocellulose fibers,” *Energy Environ. Sci.*, vol. 6, no. 2, pp. 513–518, 2013.

[39] M. Irimia-Vladu, "'Green' electronics: biodegradable and biocompatible materials and devices for sustainable future," *Chem. Soc. Rev.*, vol. 43, no. 2, pp. 588–610, 2014.

[40] P. Ihalainen, A. Määttänen, J. Järnström, D. Tobjörk, R. Österbacka, and J. Peltonen, "Influence of surface properties of coated papers on printed electronics," *Ind. Eng. Chem. Res.*, vol. 51, no. 17, pp. 6025–6036, 2012.

[41] R. Martins, A. Nathan, R. Barros, L. Pereira, P. Barquinha, N. Correia, R. Costa, A. Ahnood, I. Ferreira, and E. Fortunato, "Complementary metal oxide semiconductor technology with and on paper," *Adv. Mater.*, vol. 23, no. 39, pp. 4491–4496, 2011.

[42] "Demonstrators | CENIMAT." [Online]. Available: http://www.cenimat.fct.unl.pt/rd-id-teams/materials-electronics-optoelectronics-and-nanotechnologies/demonstrators. [Accessed: 27-Aug-2015].

[43] "Projeto europeu A3Ple na área da electrónica em papel (CEMOP/UNINOVA e CENIMAT/i3N) ganha prémio para melhor demonstrador na prestigiada LOPEC 2015 | CENIMAT." [Online]. Available: http://www.cenimat.fct.unl.pt/news/2015/03/projeto-europeu-a3ple-na-area-da-electronica-em-papel-cemopuninova-e-cenimati3n-ganha-premio-para-me. [Accessed: 27-Aug-2015].

[44] D. Marani, C. Gadea, J. Hjelm, P. Hjalmarsson, M. Wandel, and R. Kiebach, "Influence of hydroxyl content of binders on rheological properties of cerium–gadolinium oxide (CGO) screen printing inks," *J. Eur. Ceram. Soc.*, vol. 35, no. 5, pp. 1495–1504, May 2014.

[45] D. Marani, C. Gadea, J. Hjelm, P. Hjalmarsson, M. Wandel, and R. Kiebach, "Influence of hydroxyl content of binders on rheological properties of cerium–gadolinium oxide (CGO) screen printing inks," *J. Eur. Ceram. Soc.*, vol. 35, no. 5, pp. 1495–1504, May 2015.

[46] M. R. Somalu, V. Yufit, I. P. Shapiro, P. Xiao, and N. P. Brandon, "The impact of ink rheology on the properties of screen-printed solid oxide fuel cell anodes," *Int. J. Hydrogen Energy*, vol. 38, no. 16, pp. 6789–6801, 2013.

[47] S. Thomas, D. Durand, C. Chassenieux, and P. Jyotishkumar, *Handbook of Biopolymer-Based Materials*. Weinheim, Germany: Wiley-VCH Verlag GmbH & Co. KGaA, 2013.

[48] X. Qiu and S. Hu, "'Smart' materials based on cellulose: A review of the preparations, properties, and applications," *Materials (Basel).*, vol. 6, no. 3, pp. 738–781, 2013.

[49] M. Henriksson, L. a. Berglund, P. Isaksson, T. Lindström, and T. Nishino, "Cellulose nanopaper structures of high toughness," *Biomacromolecules*, vol. 9, no. 6, pp. 1579–1585, 2008.

[50] L. Hu, G. Zheng, J. Yao, N. Liu, B. Weil, M. Eskilsson, E. Karabulut, Z. Ruan, S. Fan, J. T. Bloking, M. D. McGehee, L. Wågberg, and Y. Cui, "Transparent and conductive paper from nanocellulose fibers," *Energy Environ. Sci.*, vol. 6, no. 2, p. 513, 2013.

[51] G. Siqueira, J. Bras, and A. Dufresne, "Cellulosic Bionanocomposites: A Review of Preparation, Properties and Applications," *Polymers (Basel).*, vol. 2, no. 4, pp. 728–765, Dec. 2010.

[52] Z. Wang, S. Liu, Y. Matsumoto, and S. Kuga, "Cellulose gel and aerogel from LiCl/DMSO solution," *Cellulose*, vol. 19, no. 2, pp. 393–399, Apr. 2012.

[53] T. Huber, J. Müssig, O. Curnow, S. Pang, S. Bickerton, and M. P. Staiger, "A critical review of all-cellulose composites," *J. Mater. Sci.*, vol. 47, no. 3, pp. 1171–1186, 2012.

[54] S. Zhang, F.-X. Li, J. Yu, and Y.-L. Hsieh, "Dissolution behaviour and solubility of cellulose in NaOH complex solution," *Carbohydr. Polym.*, vol. 81, no. 3, pp. 668–674, Jul. 2010.

[55] H. Koga, M. Nogi, N. Komoda, T. T. Nge, T. Sugahara, and K. Suganuma, "Uniformly connected conductive networks on cellulose nanofiber paper for transparent paper electronics," *NPG Asia Mater.*, vol. 6, no. 3, p. e93, Mar. 2014.

[56] L. Liu, Z. Niu, L. Zhang, W. Zhou, X. Chen, and S. Xie, "Nanostructured Graphene Composite Papers for Highly Flexible and Foldable Supercapacitors," *Adv. Mater.*, vol. 26, no. 28, pp. 4855–4862, Jul. 2014.

[57] H. Qi, E. Mäder, and J. Liu, "Electrically conductive aerogels composed of cellulose and carbon nanotubes," *J. Mater. Chem. A*, vol. 1, no. 34, p. 9714, 2013.

[58] C. Kim, S.-H. Park, J.-I. Cho, D.-Y. Lee, T.-J. Park, W.-J. Lee, and K.-S. Yang, "Raman spectroscopic evaluation of polyacrylonitrile-based carbon nanofibers prepared by

electrospinning," *J. Raman Spectrosc.*, vol. 35, no. 11, pp. 928–933, Nov. 2004.

[59] X. Huang, "Fabrication and Properties of Carbon Fibers," *Materials (Basel).*, vol. 2, no. 4, pp. 2369–2403, Dec. 2009.

[60] S.-J. Park, Carbon Fibers, vol. 210. Dordrecht: Springer Netherlands, 2015.

[61] E. LichaoFeng, E. NingXie, and J. Zhong, "Carbon Nanofibers and Their Composites: A Review of Synthesizing, Properties and Applications," Materials (Basel)., vol. 7, no. 5, pp. 3919–3945, May 2014.

[62] "SIGRAFIL_Short_Carbon_Fibers_e.pdf." [Online]. Available: https://www.sglgroup.com/cms/_common/downloads/products/product-groups/cf/short-carbon-fibers/SIGRAFIL_Short_Carbon_Fibers_e.pdf. [Accessed: 25-Aug-2015].

[63] S. Park, M. Vosguerichian, and Z. Bao, "A review of fabrication and applications of carbon nanotube film-based flexible electronics.," *Nanoscale*, vol. 5, no. 5, pp. 1727–52, 2013.

[64] M. Terrones, "Synthesis, Properties, and Applications of Carbon Nanotubes," *Annu. Rev. Mater. Res.*, vol. 33, no. 1, pp. 419–501, 2003.

[65] I. Cunha, "Desenvolvimento de nanofilmes à base de óxido de tungsténio para aplicações em transístores electrocrómicos," Master Thesis, Departamento de Ciências dos Materiais, FCT UNL, Portugal (2013).

[66] P. Grey, "Development of Electrochromic Thin-Film Transistors on Flexible Substrate," Master Thesis, Departamento de Ciências dos Materiais, FCT UNL, Portugal (2014).

[67] Y. A. Samad, A. Asghar, and R. Hashaikeh, "Electrospun cellulose / PEO fi ber mats as a solid polymer electrolytes for Li ion batteries," *Renew. Energy*, vol. 56, pp. 90–95, 2013.

[68] J. Zhang, L. Yue, P. Hu, Z. Liu, B. Qin, B. Zhang, Q. Wang, G. Ding, C. Zhang, X. Zhou, J. Yao, G. Cui, and L. Chen, "Taichi-inspired rigid-flexible coupling cellulose-supported solid polymer electrolyte for high-performance lithium batteries," *Sci. Rep.*, vol. 4, p. 6272, 2014.

[69] L. An, T. S. Zhao, and L. Zeng, "Agar chemical hydrogel electrode binder for fuel-electrolyte-fed fuel cells," *Appl. Energy*, vol. 109, pp. 67–71, Sep. 2013.

[70] C. Chang and L. Zhang, "Cellulose-based hydrogels: Present status and application prospects," *Carbohydr. Polym.*, vol. 84, no. 1, pp. 40–53, Feb. 2011.

[71] A. M. Ramos, S. Pereira, M. T. Cidade, G. Pereira, R. Branquinho, L. Pereira, R. Martins, and E. Fortunato, "Preparation and characterization of cellulose nanocomposite hydrogels as functional electrolytes," *Solid State Ionics*, vol. 242, pp. 26–32, 2013.

[72] S. Tabanli, A. Gelir, and Y. Yilmaz, "Polyacrylamide hydrogel as an electrolyte for oxidation-based organic rectifiers," *Polym. Eng. Sci.*, vol. 55, no. 2, pp. 406–413, Feb. 2015.

[73] L. Santos, D. Nunes, T. Calmeiro, R. Branquinho, D. Salgueiro, P. Barquinha, L. Pereira, R. Martins, and E. Fortunato, "Solvothermal Synthesis of Gallium–Indium-Zinc-Oxide Nanoparticles for Electrolyte-Gated Transistors," *ACS Appl. Mater. Interfaces*, vol. 7, no. 1, pp. 638–646, Jan. 2015.

[74] Y. Masuda, Y. Jinbo, and K. Koumoto, "Room Temperature CVD of TiO₂ Thin Films and Their Electronic Properties," *Sci. Adv. Mater.*, vol. 1, no. 2, pp. 138–143, Aug. 2009.

[75] Qiang Lu, R. Lin, H. Takeuchi, Tsu-Jae King, Chenming Hu, K. Onishi, Rino Choi, Chang-Seok Kang, and J. C. Lee, "Deep-submicron CMOS process integration of HfO/sub 2/ gate dielectric with poly-Si gate," in *2001 International Semiconductor Device Research Symposium. Symposium Proceedings (Cat. No.01EX497)*, pp. 377–380.

[76] R. Puthenkovilakam, E. a. Carter, and J. P. Chang, "First-principles exploration of alternative gate dielectrics: Electronic structure of ZrO2/Si and ZrSiO4/Si interfaces," *Phys. Rev. B*, vol. 69, no. 15, p. 155329, Apr. 2004.

[77] M. B. Vázquez-Santos, E. Geissler, K. László, J.-N. Rouzaud, A. Martínez-Alonso, and J. M. D. Tascón, "Comparative XRD, Raman, and TEM Study on Graphitization of PBO-Derived Carbon Fibers," *J. Phys. Chem. C*, vol. 116, no. 1, pp. 257–268, Jan. 2012.

[78] A I. López-Lorente, B. M. Simonet, and M. Valcárcel, "Qualitative detection and quantitative determination of single-walled carbon nanotubes in mixtures of carbon nanotubes with a portable

Raman spectrometer," *Analyst*, vol. 138, no. 8, p. 2378, 2013.

[79] J.-P. Tessonnier, D. Rosenthal, T. W. Hansen, C. Hess, M. E. Schuster, R. Blume, F. Girgsdies, N. Pfänder, O. Timpe, D. S. Su, and R. Schlögl, "Analysis of the structure and chemical properties of some commercial carbon nanostructures," *Carbon N. Y.*, vol. 47, no. 7, pp. 1779–1798, Jun. 2009.

[80] J. Arenales Rivera, V. Pérez López, R. Ramos Casado, and J.-M. Sánchez Hervás, "Thermal degradation of paper industry wastes from a recovered paper mill using TGA. Characterization and gasification test," *Waste Manag.*, May 2015.

[81] V. Mangut, E. Sabio, J. Gañán, J. F. González, A. Ramiro, C. M. González, S. Román, and A. Al-Kassir, "Thermogravimetric study of the pyrolysis of biomass residues from tomato processing industry," *Fuel Process. Technol.*, vol. 87, no. 2, pp. 109–115, Jan. 2006.

[82] C. Zhou, W. Yang, and W. Blasiak, "Characteristics of waste printing paper and cardboard in a reactor pyrolyzed by preheated agents," *Fuel Process. Technol.*, vol. 116, no. August, pp. 63–71, Dec. 2013.

[83] A. Sanson, P. Mangifesta, and E. Roncari, "Environmental-friendly screen printing ink for gas sensors," no. September, pp. 825–830, 2015.

[84] R. Alias and S. Mohd, "Rheological Behaviors and Their Correlation with Printing Performance of Silver Paste for LTCC Tape," in *Rheology*, InTech, 2012.

[85] F. D. Barlow, A. Elshabini, and A. K. Knudsen, "Multilayer Ceramics," in *Ceramic Interconnect Technology Handbook*, CRC Press, 2007.

[86] K. Inukai, Y. Takahashi, K. Ri, and W. Shin, "Rheological analysis of ceramic pastes with ethyl cellulose for screen-printing," *Ceram. Int.*, vol. 41, no. 4, pp. 5959–5966, May 2015.

[87] A. Sanson, E. Roncari, S. Boldrini, P. Mangifesta, and L. Doubova, "Eco-Friendly Screen-Printing Inks of Gadolinia Doped Ceria," *J. Fuel Cell Sci. Technol.*, vol. 7, no. 5, p. 051013, 2010.

[88] S. El-Sayed, K. H. Mahmoud, A. A. Fatah, and A. Hassen, "DSC, TGA and dielectric properties of carboxymethyl cellulose/polyvinyl alcohol blends," *Phys. B Condens. Matter*, vol. 406, no. 21, pp. 4068–4076, Nov. 2011.

[89] O. A. Cavalcanti, B. Petenuci, A. C. Bedin, E. a G. Pineda, and a. a W. Hechenleitner, "Characterisation of Ethylcellulose Films containing Natural Polysaccharides by Thermal Analysis and FTIR Spectroscopy," *Acta Farm. Bonaer.*, vol. 23, no. 1, pp. 53–57, 2004.

[90] J. Desai, K. Alexander, and A. Riga, "Characterization of polymeric dispersions of dimenhydrinate in ethyl cellulose for controlled release," *Int. J. Pharm.*, vol. 308, no. 1–2, pp. 115–123, Feb. 2006.

[91] R. M. Serra, E. E. Miró, and A. V. Boix, "FTIR study of toluene adsorption on Cs-exchanged mordenites," *Microporous Mesoporous Mater.*, vol. 127, no. 3, pp. 182–189, Feb. 2010.

[92] A M. Adel, A M. Nada, H. Abou-Youssef, and a. a. El-Gendy, "Carboxymethylated Cellulose Hydrogel ; Sorption Behavior and Characterization," *Nat. Sci.*, vol. 8, no. 8, pp. 244–256, 2010.

[93] M. N. Chai and M. I. N. Isa, "The Oleic Acid Composition Effect on the Carboxymethyl Cellulose Based Biopolymer Electrolyte," *J. Cryst. Process Technol.*, vol. 03, no. 01, pp. 1–4, 2013.

[94] S. Wang and D. D. L. Chung, "Electrical behavior of carbon fiber polymer-matrix composites in the through-thickness direction," *J. Mater. Sci.*, vol. 35, no. 1, pp. 91–100, 2000.

[95] P. B. P. Jana, S. Chaudhuri, a. K. Pal, and S. K. De, "Electrical conductivity of short carbon fiber reinforced polychloroprene rubber and mechanism of conduction," *Polym. Eng. …*, vol. 32, no. 6, pp. 448–456, 1992.

[96] L. Herlogsson, *Electrolyte-Gated Organic Thin-Film Transistors*. 2011.

[97] M. J. Rodíguez Presa, R. I. Tucceri, M. I. Florit, and D. Posadas, "Constant phase element behavior in the poly(o-toluidine) impedance response," *J. Electroanal. Chem.*, vol. 502, no. 1–2, pp. 82–90, Apr. 2001.

7. ANNEX

Annex A - Squematic of a home made screen printing stage (Adapted from [35]).

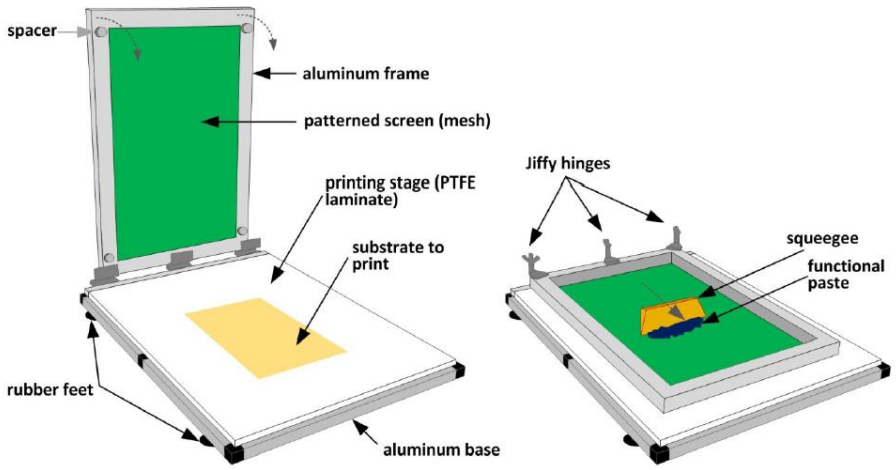

Annex B - Typical shear rate values of each printing stage and typical viscosity values for screen printing technique. [84]

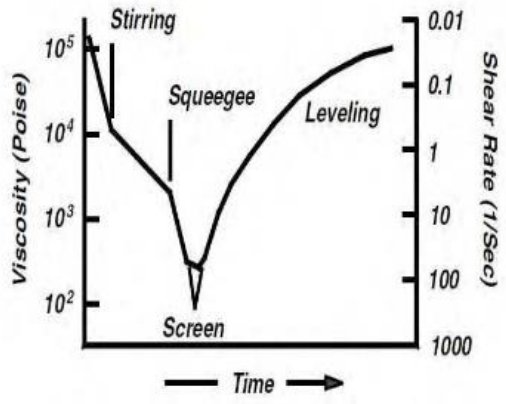

Annex C – Schematic of fabrication steps of CFs provided by FISIPE. The CF precursor is PAN is subjected to an oxidation step under 200-300 ºC followed by the carbonization under 1200-1400 ºC. After that, carbon ribbons are subjected to a surface treatment, winded up and milled into fibers. [62]

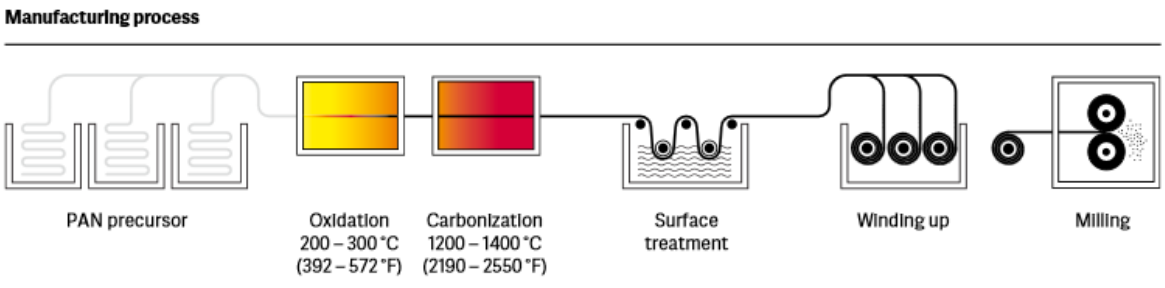

Annex D –Structure of single (SWCNT) and multi-walled carbon nanotubes (MWCNT). On the top, wraping of a single graphene foil to form SWCNTs and on the bottom wrapping up several graphene foils results in MWCNTs.

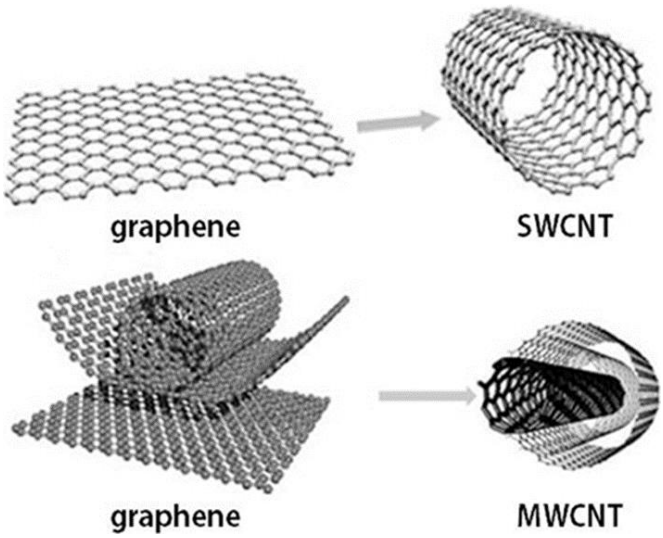

Annex E – Carbon structures samples preparations for SEM:

The CFs samples preparation consisted of spreading a small amount of powder on the surface of a carbon tape. The MWCNTs were first dispersed in an aqueous solution with Triton-X100, ultrasonicated in a UP400S sonicator for 30 min with a cylindrical tip (3 mm end cap diameter), using the folling parameters: amplitude, 40 %; time on, 2 s; time off, 2 s. A droplet was casted on the carbon tape and dried overnight for solvent evaporation. Finally, the samples were coated with a thin iridium layer(~ 15 nm thickness) using a Q300T D Quorum sputtering system.

Annex F - Formulation and nomenclature of CFs based electroconductive inks. Weight percentage (wt. %) of each component used to prepare the cellulose-based electroconductive inks, using distinct CFs (pristine and milled).

Cellulose derivative	Solvent	CFs concentration (% wt.)	Mechanical treatment implemented to the CFs
CMC (3 % wt.)	Deionized water	5	None
			Milling
		10	None
			Milling
EC (5 % wt.)	Ethanol:toluene (20:80 %v/v)	5	None
			Milling
		10	None
			Milling

Annex G - Formulation and nomenclature of MWCNTs based electroconductive inks. Weight percentage (wt. %) of each component used to prepare the cellulose-based electroconductive inks, using MWCNTs.

Cellulose derivative	Solvent	MWCNTs concentration (wt%)
CMC (3 % wt.)	Deionized water	0.1
		0.5
EC (5 % wt.)	Ethanol:toluene (20:80 %v/v)	5
		10

Annex H – Formulation and nomenclature of electrolytes. Weight percentage (% wt.) of each component used to prepare hydrogel electrolytes, before neutralization step.

Nomenclature	MCC concentration (% wt.)	Dissolution
MCC4	4	LiOH/U/H_2O (4.6/15/80.4 %wt.)
MCC8	8	

Annex I - Schematic representation of top view and cross section (CS) of each layer of EGTs with a W/L = 950/190: Metallic contacts of Ti/Au of 6/60 nm thick deposited by e-beam evaporation (a); GIZO semiconducting layer of 35 nm thick, deposited by RF magnetron sputtering (b); Hydrogel electrolyte deposited by drop casting (c).

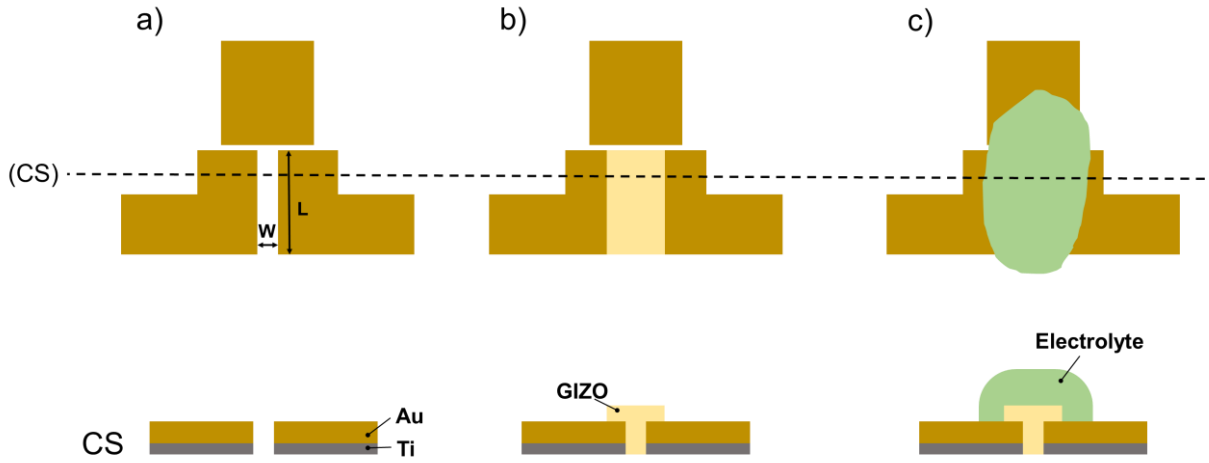

Annex J – Expression used to calculate resistivity [40]:

$$\rho = R\frac{A}{l} \quad (1)$$

Where ρ is the resistivity (Ωcm), l is the length size of the CFs (cm), and A is the transversal area (cm^2).

Annex K – Pattern used to study resolution of inks.

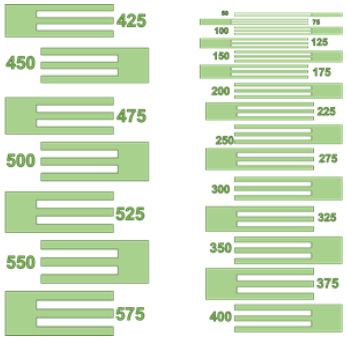

Annex L – Definition on patterns obtained from EC at 5 % wt. (a) and CMC at 3 % wt. (b) solutions.

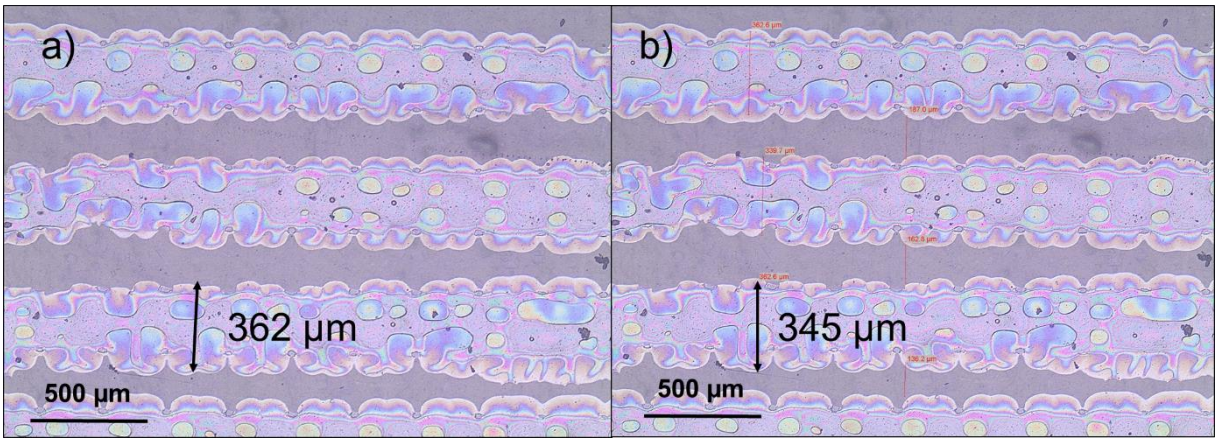

Annex M – FTIR –ATR spectra of ultrapure water with major peak identified at 3264 cm^{-1}.

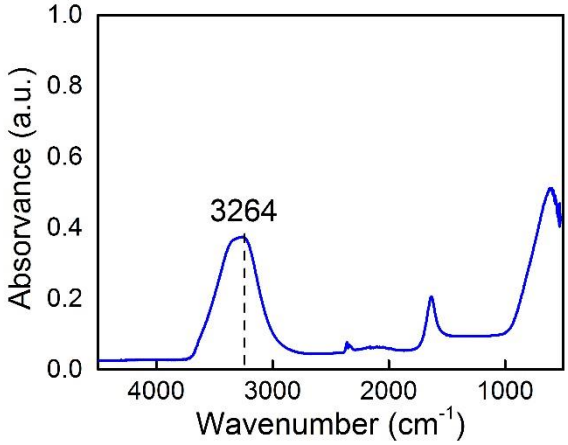

Annex N - CMC3 CF10 ink (a). MCC4 (b) and MCC8 (c) hydrogel electrolytes.

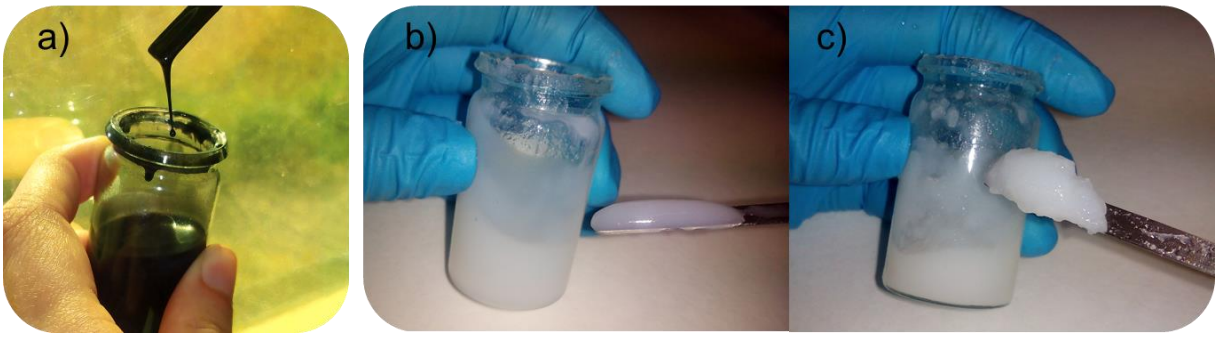

Annex O – Thickness of screen printed films from CMC3 CF10 ink selected samples with 10 layers.

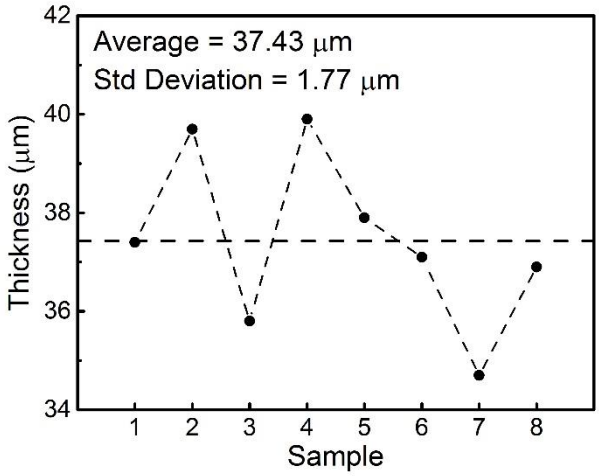

Annex P – Expression used to calculate sheet resistance [85]:

$$R_{\square} = \frac{\rho}{t} \qquad (1)$$

Where $R_{\square}$ is the sheet resistance ($\Omega/\square$), ρ is the resistivity (Ωcm) and t is the thickness (cm).

Annex Q - DSC analysis of a CMC membrane. The frst mass loss of 18.08 % steps. corresponds to evaporation of adsorbed water on the cellulosic matrix.

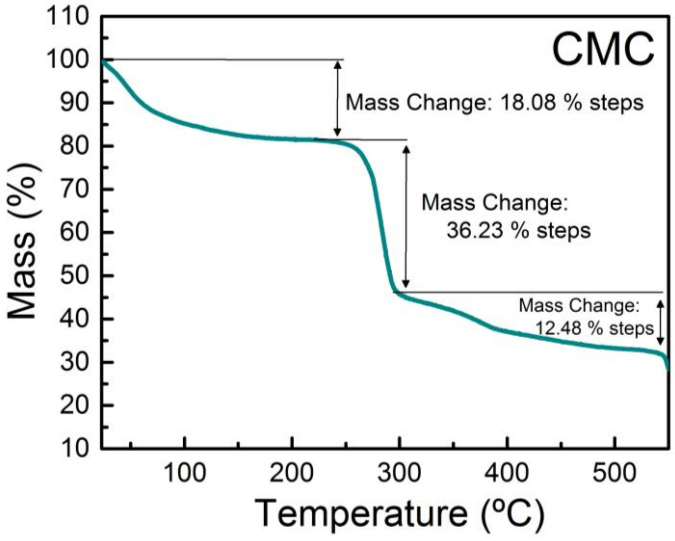

Annex R – Reprensentation of the logaritm of conductivity versus the inverse value of temperature and linear regression on the two aparent conduction regims observed.

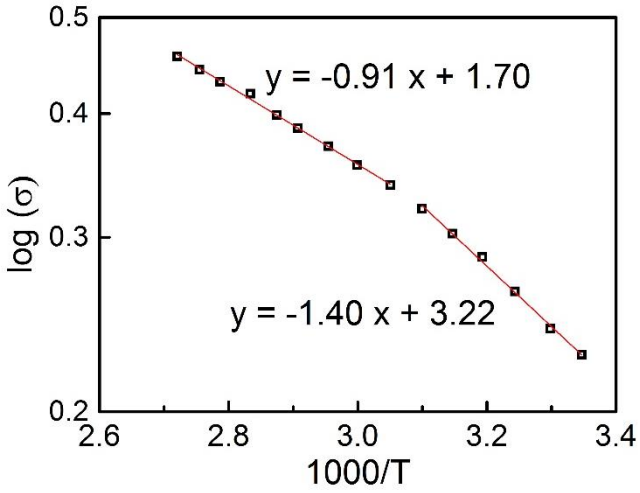

Annex S – Expression used to calculate activation energy [94] :

$$\sigma = \sigma_0 \ln\left(\frac{-\mathrm{E_a}}{K_B T}\right) \qquad (2)$$

Where σ is the conductivity ($\Omega^{-1}cm$), σ_0 is the pre-exponential factor, $\mathrm{E_a}$ is the activation energy (eV), K_B is the Boltzmann constant (8.617x10-5 eV/K) and T is the temperature (K).

Annex T– Schematic representation of ionic and potential distribution on double layer formed in electrolyte when an external potential is applied, as described by CGS model. [96]

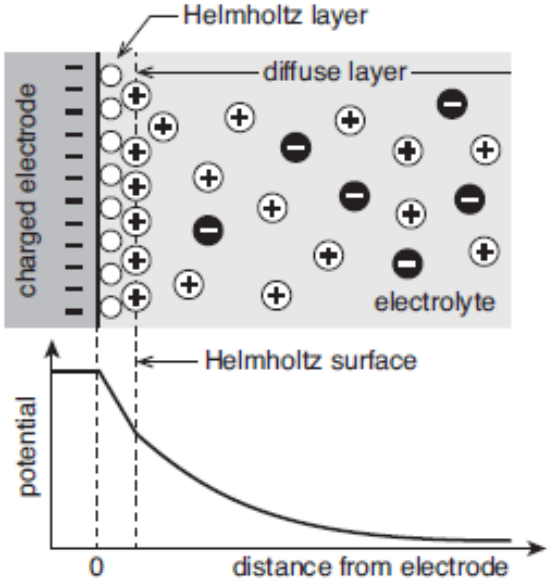

Annex U – Parameters obtained from fitting to obtained data with the Rendel fitting of data from Figure 4.28.

	MCC4		MCC8	
	Value	**Error**	**Value**	**Error**
Thickness (μm)	421	-	1087	-
Area (cm^2)	0.994	-	0.994	-
R_b (Ω)	1.19×10^5	8.87×10^3	1.96×10^5	5.76×10^3
R_{ext} (Ω)	2.47×10^1	1.52×10^{-1}	1.49×10^2	9.08×10^{-1}
Y_0 (Fcm^{-1})	4.53×10^{-5}	3.91×10^{-7}	9.67×10^{-6}	8.85×10^5
α	8.37×10^{-1}	1.82×10^{-3}	8.33×10^{-1}	1.94×10^{-3}
Goodness of fitting	2.21×10^{-3}	-	8.66×10^{-4}	-
C_{DL} (μF)	1.21×10^1	-	2.61×10^0	-
C_{DL}/A (μFcm^{-2})	1.22×10^1	-	2.62×10^0	-
σ_i (Scm^{-1})	3.56×10^{-7}	-	5.57×10^{-7}	-

Annex V – Expression used to calculate double layer capacitance (C_{DL}) of electrolytes [73]:

$$C_{DL} = [\mathrm{Y}_0 \mathrm{R}_{ext}{}^{-(\alpha-1)}]^{1/\alpha} \quad (3)$$

Where C_{DL} is the double layer capacitance (Fcm^{-1}), Y_0 is the bulk capacitance (Fcm^{-1}), R_{ext} is the contact resistance (Ω) and α is the ideality of capacitive behaviour constante (between 0 and 1).

Annex W - Expression used to calculate ionic conductivity (σ_i) of electrolytes [73]:

$$\sigma_i = \frac{l}{R_b A} \quad (4)$$

Where σ_i is the ionic conductivity ($\Omega^{-1}cm$), l is the thickness of electrolyte (cm), R_b is the bulk resistance (Ωcm), A is the area of electrodes (cm^2).

Annex X - Expression used calculate mobility in linear regime [73]:

$$\mu_{LIN} = \frac{\left(\frac{dI_D}{dV_G}\right)}{C\frac{W}{L}V_D} \quad (5)$$

Where μ_{LIN} is the mobility ($cm^2V^{-1}s^{-1}$), I_D is the drain current (A), V_G is the gate voltage (V), C is the capacitance (Fcm^{-1}), W is the width (μm), L is the length (μm), V_D is the drain voltage (V).

Annex Y - Expression used calculate mobility in linear regime [73]:

$$SS = \left(\frac{d \log(\mathrm{I_D})}{dV_G} \bigg|_{\max} \right)^{-1} \quad (6)$$

Where SS is the subtreshold voltage (V / dec), $\mathrm{I_D}$ is the drain current (A) and V_G .is ths gate voltage (V).

Annex Z - Expression used calculate transconductance [66]:

$$g_m = \frac{dI_D}{dV_G} \quad (7)$$

Where g_m is the transconductance (S), $\mathrm{I_D}$ is the drain current (A), V_G is the gate voltage (V).